Maria Sklodowska Curie Actions - Research and Innovation Staff Exchange

H2020-MSCA-RISE-2020 - SAFEMILK, project No. 101007299

Report on the
International school
Surface modification and application of electrochemical and acoustic techniques for detection of affinity interactions at surfaces

The International school has been organized by Comenius University in Bratislava, Slovakia on May 30 - June 2, 2022, in framework of SAFEMILK project. The school has been divided on 3 parts: 1. Tutorial lectures presented by 7 internationally recognized scientists 2. The workshop “Biosensors in food safety” took place on May 31, 2022, and consisted in 5 invited lectures and 9 short communications. The tutorial lectures and the workshop were organized remotely through MS Teams platform 3. Practical courses have been organized on site at the Department of Nuclear Physics and Biophysics, Faculty of Mathematics, Physics, and Informatics of Comenius University in Bratislava on June 1-2, 2022. The International school has been very successful. 61 participants from 10 European countries (Belgium, Czech Republic, Greece, Hungary, France, Italy, Portugal, Turkey, Slovakia, UK) as well as from Canada, China, India, UK, and USA attended the school, of which 16 attended the practical courses. The tutorial lectures were focused on the introduction to the fundamentals of electrochemical and acoustics biosensors as well as on the principles of electrochemical impedance spectroscopy, surface modification, application of nanostructures in the biosensor development, application of DNA aptamers in development of biosensors for monitoring of food contamination as well as on the principles of electromagnetic piezoelectric acoustics sensors and importance of the preparation of sensing surfaces with antifouling properties. The invited lectures at the workshop have been concentrated on the application of biosensor technology for food safety. At most of the short oral communications the participants presented results obtained during the secondments.

Practical courses consisted of 5 tasks focused on obtaining experience in the preparation of aptamer-based biosensors and for application of amperometry and electrochemical impedance spectroscopy for detection affinity interactions at surfaces. The task on application of quartz crystal microbalance with dissipation (QCM-D) demonstrated the possibility of this method in analysis of various surface modifications and to study the molecular interactions at surfaces. There were also tasks focused on application of gold nanoparticles in colorimetry and in the characterization of the size and zeta potential due to various modifications.

Enclosed below is list of participants, and list of attendance of practical courses. The detailed information about the program and the practical tasks is in enclosed book of abstracts and practical courses.

Prof. Tibor Hianik
School organizer

Bratislava, June 7, 2022

Maria Sklodowska Curie Actions - Research and Innovation Staff Exchange
H2020-MSCA-RISE-2020 - SAFEMILK

International School
Surface modification and application of electrochemical and acoustic techniques for detection of affinity interactions at surfaces

List of participants

No	Surname, name, title	Category	Institute/e-mail
1	Csiba Martin, Bc.	ESR	Comenius University, Bratislava Slovakia/csiba17@uniba.sk
2	Garaiová Zuzana, Dr.	ER	Comenius University, Bratislava Slovakia/garaiova.zuzana7@gmail.com
3	Hianik Tibor, prof.	ER	Comenius University, Bratislava Slovakia/ tibor.hianik@fmph.uniba.sk
4	Mikuličová Sára, Ms.	ESR	Comenius University, Bratislava Slovakia/ mikulicova6@uniba.sk
5	Oravczová Veronika, Mgr.	ESR	Comenius University, Bratislava Slovakia/ oravczova.v@gmail.com
6	Piovarči Ivan, Mgr.	ESR	Comenius University, Bratislava Slovakia/piovarci.i@gmail.com
7	Spagnolo Sandro, Dr.	ER	Comenius University, Bratislava Slovakia/ sandrospagnolo1@gmail.com
8	Šubjaková Veronika, Dr.	ER	Comenius University, Bratislava Slovakia/subjakov@gmail.com
9	Tatarko Marek, Dr.	ER	Comenius University, Bratislava Slovakia/mtatarko1@gmail.com
10	Waczulíková Iveta, Assoc.Prof.	ER	Comenius University, Bratislava Slovakia/ iveta.waczulikova@fmph.uniba.sk
11	Bousiakou Lida, Dr.	ER	IMD Laboratories, Athens, Greece/ leda07@hotmail.com
12	Karapetis Stefanos, Dr.	ER	IMD Laboratories, Athens, Greece/ tvikaria@gmail.com
13	Economou Anastasios, prof.	ER	National Kapodistrian University of Athens, Greece/ aeconomo@chem.uoa.gr
14	Melios Nikitas, MSc.	ESR	National Kapodistrian University of Athens, Greece/ nikitasmelios@yahoo.gr
15	Pgakali Varvara, Dr.	ER	National Kapodistrian University of Athens, Greece/ bpagali@yahoo.gr
16	Tsekenis George, Dr.	ER	Biomedical Research Foundation of the Academy of Athens, Greece/ gtsekenis@bioacademy.gr
17	Angelopoulou Michailia, Dr.	ER	NCSR “Demokritos”, Athens, Greece/ mikangelchem@gmail.com
18	Geka Georgia, MSc.	ESR	NCSR “Demokritos”, Athens, Greece/georgia.geka101@gmail.com
19	Kakabakos Sotirios, Dr	ER	NCSR “Demokritos”, Athens, Greece/skakab@rrp.demokritos.gr
20	Kanioura Anastasia, Dr.	ER	NCSR “Demokritos”, Athens, Greece/kaniourita@yahoo.gr
21	Kourti, Dimitra, MSc.	ESR	NCSR “Demokritos”, Athens, Greece/dimkourti96@gmail.com
22	Livaniou Evangelia, Dr.	ER	NCSR “Demokritos”, Athens, Greece/livanlts@rrp.demokritos.gr
23	Petrou Panagiota, Dr.	ER	NCSR “Demokritos”, Athens, Greece/ ypetrou@rrp.demokritos.gr
24	Gizeli Electra, prof.	ER	University of Crete, Greece/gizeli@imbb.forth.gr
25	Bakos István, Dr.	ER	Research Centre for Natural Sciences, Budapest, Hungary/ bakos.istvan@ttk.hu
26	Csanádi Laura, MSc.	ER	Research Centre for Natural Sciences, Budapest, Hungary/ csanadi.laura@ttk.hu
27	Felhősi Ilona, Dr.	ER	Research Centre for Natural Sciences, Budapest, Hungary/felhosi.ilona@ttk.hu
28	Jakab Kristóf, MSc.	ESR	Research Centre for Natural Sciences, Budapest, Hungary/ jakab.kristof@ttk.hu

29	Keresztes Zsofia, Dr.	ER	Research Centre for Natural Sciences, Budapest, Hungary/ keresztes.zsofia@ttk.hu
30	Marek Tamás, Dr.	ER	Research Centre for Natural Sciences, Budapest, Hungary/ marek.tamas@ttk.hu
31	Meszáros Gábor, Dr.	ER	Research Centre for Natural Sciences, Budapest, Hungary/ meszaros.gabor@ttk.hu
32	Pávai Mária, MSc.	ER	Research Centre for Natural Sciences, Budapest, Hungary/ pavai.maria@ttk.hu
33	Románszki Loránd, Dr.	ER	Research Centre for Natural Sciences, Budapest, Hungary/ romanszki.lorand@ttk.hu
34	Shaban Abdul, Dr.	ER	Research Centre for Natural Sciences, Budapest, Hungary/ shaban.abdul@ttk.hu
35	Szabó Tamás, Dr.	ER	Research Centre for Natural Sciences, Budapest, Hungary/ szabo.84.tamas@ttk.hu
36	Süle Judit, Dr.	ER	Hungarian Dairy Research Institute, Mosonmagyarovar, Hungary/
37	Čapková Magdalena, Ing.	ESR	Institute of Photonics and Electronics, Prague, Czech Republic/ capkova@ufe.cz
38	Lopez Mora Nestor, Dr.	ER	J. Heyrovsky Institute of Physical Chemistry, Prague, Czech Republic/ nestor.mora@jh-inst.cas.cz
39	Scollo Federica, MSc.	ESR	J. Heyrovsky Institute of Physical Chemistry, Prague, Czech Republic/ federica.scollo@jh-inst.cas.cz
40	Butera Ester, MSc	ESR	Università degli studi di Catania, Italy/ester.butera@gmail.com
41	Maccarrone Giuseppe, prof.	ER	Università degli studi di Catania, Italy/ gmacca@unict.it
42	Tong Liu, Ms.	ESR	Charles University, Prague, Czech Republic/ liu@ufe.cz
43	Galicová Tatiana, Ing.	ESR	Institute of Biophysics, Brno Czech Republic/ galicova@ibp.cz
44	Ostatná Veronika, Dr.	ER	Institute of Biophysics, Brno Czech Republic/ ostatna@ibp.cz
45	Brett Christopher, prof	ER	University of Coimbra, Portugal/ cbrett@ci.uc.pt
46	Marty Jean Louis, prof.	ER	University of Perpignan, France/ jlmarty@univ-perp.fr
47	Erdem Arzum, prof.	ER	Ege University, Izmir, Turkey/ arzum.erdem@ege.edu.tr
48	Meltem Maral, Bc.	ESR	Ege University, Izmir, Turkey/ meltemmaral58@gmail.com
49	Senturk Huseyin, MSc.	ESR	Ege University, Izmir, Turkey/ mhuseyinsenturk@hotmail.com
50	Yildiz Esma, MSc.	ESR	Ege University, Izmir, Turkey/ esmayildiz94@gmail.com
51	Shirsat Mahendra, prof.	ER	Dr. Babasaheb Ambedkar Marathwada University, Aurangabad, India/ mdshirsat.phy@bamu.ac.in
52	Sontakke Kiran, MSc.	ESR	Dr. Babasaheb Ambedkar Marathwada University, Aurangabad, India/ kiransontakke07@gmail.com
53	Wang Feng, Dr.	ER	Zhongkai University of Agriculture and Engineering, Guangzhou, China/ wangfeng_sp@163.com
54	Wang Joseph, prof.	ER	University of California San Diego, USA/ josephwang@ucsd.edu
55	Thompson Michael, prof.	ER	University of Toronto, Canada/ m.thompson@utoronto.ca
56	Ivanov Ilia N., prof.	ER	CNMS, Oak Ridge National laboratory, USA/ ivanovin@ornl.gov
57	Hanic Michal, Ing.	ER	Powertec Ltd., Bratislava, Slovakia/michal.hanic@powertec.sk
58	Szobolovsky Robert, Ing.	ER	Powertec Ltd., Bratislava, Slovakia/ robert.szobolovsky@powertec.sk
59	Vincze Tomáš, Ing	ESR	Powertec Ltd., Bratislava, Slovakia/tomas.vincze@powertec.sk
60	Psoma Sotiria, Dr.	ER	The Open University, Milton Keynes, UK/ sotiria.psoma@open.ac.uk
61	Jacquin Thierry, Dr.	REA	Research and Executive Agency, EU, Brussels, Belgium/ thierry.jacquin@ec.europa.eu

ESR – early stage researcher, ER- experienced researcher, REA – European Research Executive Agency

Maria Sklodowska Curie Actions - Research and Innovation Staff Exchange
H2020-MSCA-RISE-2020 - SAFEMILK

International School
Surface modification and application of electrochemical and acoustic techniques for detection of affinity interactions at surfaces

Attendance on practical courses

No	Surname, name, title	Category	Institute/e-mail	Signature
1	Csiba Martin, Bc	ESR	Comenius University, Bratislava Slovakia/csiba17@uniba.sk	
2	Garaiová Zuzana, Dr.	ER	Comenius University, Bratislava Slovakia/garaiova.zuzana7@gmail.com	
3	Oravczová Veronika, Mgr.	ESR	Comenius University, Bratislava Slovakia/ oravczova.v@gmail.com	
4	Piovarči Ivan, Mgr.	ESR	Comenius University, Bratislava Slovakia/piovarci.i@gmail.com	
5	Šubjaková Veronika, Dr.	ER	Comenius University, Bratislava Slovakia/subjakov@gmail.com	
6	Tatarko Marek, Dr.	ER	Comenius University, Bratislava Slovakia/mtatarko1@gmail.com	
7	Karapetis Stefanos, Dr.	ER	IMD Laboratories, Athens, Greece/ tvikaria@gmail.com	
8	Melios Nikitas, MSc.	ESR	National Kapodistrian University of Athens, Greece/ nikitasmelios@yahoo.gr	
9	Jakab Kristóf, MSc.	ESR	Research Centre for Natural Sciences, Budapest, Hungary/ jakab.kristof@ttk.hu	
10	Románszki Loránd, Dr.	ER	Research Centre for Natural Sciences, Budapest, Hungary/ romanszki.lorand@ttk.hu	
11	Szabó Tamás, Dr.	ER	Research Centre for Natural Sciences, Budapest, Hungary/ szabo.84.tamas@ttk.hu	
12	Čapková Magdalena, Ing.	ESR	Institute of Photonics and Electronics, Prague, Czech Republic/ capkova@ufe.cz	
13	Davidović David, MSc.	ESR	J. Heyrovsky Institute of Physical Chemistry, Prague, Czech Republic/ david.davidovic@jh-inst.cas.cz	
14	Lopez Mora Nestor, Dr.	ER	J. Heyrovsky Institute of Physical Chemistry, Prague, Czech Republic/ nestor.mora@jh-inst.cas.cz	
15	Scollo Federica, MSc.	ESR	J. Heyrovsky Institute of Physical Chemistry, Prague, Czech Republic/ federica.scollo@jh-inst.cas.cz	
16	Butera Ester, MSc	ESR	Università degli studi di Catania, Italy/ester.butera@gmail.com	
17	Tong Liu, Ms.	ESR	Charles University, Prague, Czech Republic/ liu@ufe.cz	

ESR – early stage researcher, ER- experienced researcher

Maria Sklodowska Curie Actions - Research and Innovation
Staff Exchange

H2020-MSCA-RISE-2020 - SAFEMILK

International School

Surface modification and application of electrochemical and acoustic techniques for detection of affinity interactions at surfaces

Program, Abstracts and Practical Courses

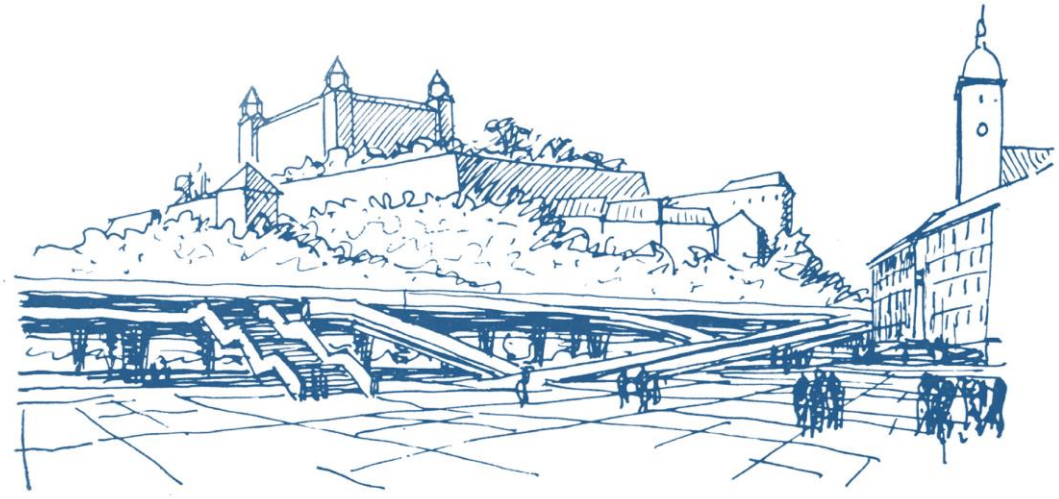

Bratislava, May 30 – June 2, 2022

Picture at the cover page: View on the Bratislava castle and St. Martin Cathedral.
Author: prof. Emanuel Hruška

International School

Surface modification and application of electrochemical and acoustic techniques for detection of affinity interactions at surfaces

Bratislava, Slovakia
May 30 – June 2, 2022

Program, Abstracts and Practical Courses

Organized by Faculty of Mathematics, Physics and Informatics, Comenius University in Bratislava
http://www.fmph.uniba.sk

in framework of

Marie Sklodowska-Curie Actions (MSCA)
Research and Innovation Staff Exchange (RISE)
H2020-MSCA-RISE-2020
SAFEMILK, Project No. 101007299
https://www.safemilkproject.com

The aim of the school is to provide a platform for introduction and training into the electrochemical and acoustics methods in the study of affinity interaction at surfaces with focus on DNA aptamers as receptors. The school will consist in the tutorial lectures of leading scientists, workshop “Biosensors in food safety” and training courses. The tutorial lectures will be focused on the introduction into the various methods used in biosensor development such as voltamperometry, impedance spectroscopy, multiharmonic quartz crystal microbalance with dissipation (QCM-D), preparation of nanoparticles and their characterization, introduction into the colorimetry based on gold nanoparticles. The courses will also include the training in the methods of the surface modification by DNA aptamers.

School is organized in framework of the project ”Innovative technology for milk safety” (SAFEMILK) funded by European Commission under the programme H2020-MCSA-RISE-2022, Project No. 101007299.
.

The International school is open for students and researchers working in bioanalysis, biophysics, electrochemistry, analytical chemistry, and related disciplines.

ORGANIZING COMMITTEE

Tibor Hianik - chairman (E-mail: tibor.hianik@fmph.uniba.sk)
Zuzana Garaiová
Maria Hianiková
Veronika Oravczová
Ivan Piovarči
Veronika Šubjaková
Marek Tatarko

Table of Content

PROGRAM

Monday, May 30, 2022
Tutorial lectures

Online - MS Teams

09:50-10:00 **Prof. Tibor Hianik**, Welcome and introduction
10:00-10:45 **T1: Prof. Anastasios Economou**, Voltammetric DNA biosensing using nanomaterial-based labels
10:45-11:30 **T2: Prof. Jean Louis Marty,** Food security: Innovative approaches based on apta-sensors and apta-assays for the detection of mycotoxins
11:30-12:15 **T3: Prof. Christopher M.A. Brett,** Electrochemical impedance spectroscopy: fundamentals and applications to sensors and biosensors

12:15-13:30 Break

13:30-14:15 **T4: Prof. Electra Gizeli**, Employing acoustic wave biosensors for applications in healthcare and agro/food safety
14:15-15:00 **T5: Prof. Michael Thompson,** Antifouling surface chemistry on acoustic wave devices

15:00-15:15 Break

15:15-16:00 **T6: Prof. Ilia Ivanov,** From the detection of an acoustic signature of event to impactful applications
16:00-16:45 **T7: Prof. Joseph Wang,** Micromotors go *in vivo*: From the bench to the body

Tuesday, May 31, 2022
Workshop „Biosensors in food safety“

Online MS Teams

Invited lectures

10:00-10:30 **IL1: Dr. Feng Wang,** Nanobodies for accurate detection of small-molecule contaminants in food
10:30-11:00 **IL2: Prof. Mahendra Shirsat,** Peptides functionalized conducting polymer-graphene OFETs for detection of aqueous phase pollutants
11:00-11:30 **IL3: Dr. Panagiota Petrou,** Applications of optical immunosensors to food safety
11:30-12:00 **IL4: Dr. Veronika Ostatná,** Electrochemical sensing of glycoproteins at charged surfaces

12:00-14:00 Break

14:00-14:30 **IL5: Prof. Arzum Erdem,** Electrochemical aptasensors developed for detection of biointeractions

Short Communications

14:30-14:45 **SC1: Nikitas Melios,** Low-cost, AChE-based, electrochemical sensors for pesticide detection in vegetable oils: sensor fabrication methodology and measurement matrix effects on sensor performance
14:45-15:00 **SC2: Kiran Sontakke,** Detection of cadmium in aqueous medium by electrochemical method
15:00-15:15 **SC3: Magdalena Čapková**, Surface plasmon resonance biosensor for detection of tramadol in drinking water
15:15-15:30 **SC4: Federica Scollo**, Galectin-1 binding to model lipid membrane investigated by the combination of QCM-D and fluorescence methods

15:30-15:45 Break

15:45-16:00 **SC5: Veronika Oravczová**, Application of electrochemical biosensors and DNA aptamers for the detection of pathogenic bacteria
16:00-16:15 **SC6: Ivan Piovarči**, Aptamer-modified gold nanoparticles in colorimetric detection of *E. coli*
16:15-16:30 **SC7: Dr. Sandro Spagnolo**, Detection of *Escherichia coli* in milk by a piezoelectric aptasensor with an anti-fouling coating
16:30-16:45 **SC8: Dr. Stefanos Karapetis**, Electrochemical detection of penicillin G and aflatoxin M1 using redox tagged DNA aptamers
16:45-17:00 **SC9: Dr. Marek Tatarko,** Detection of bacterial pathogens using multiharmonic acoustic methods and determination of their viscoelastic properties

17:00 **Conclusion**

Wednesday, June 1, 2022

09:00-10:00 Introduction to the practical courses (FMFI UK, Room F1-326)

Practical Courses

June 1-2, 2022

FMFI UK, rooms F1-342, F1-347 and F1-350
10:00-17:00

Abstracts of Tutorial Lectures

T1
Voltammetric biosensing using nanomaterial-based labels

Anastasios Economou*

Department of Chemistry, National and Kapodistrian University of Athens, Panepistimiopolis, Athens 157 71, Greece
** Corresponding author: aeconomo@chem.uoa.gr*

Methods that enable sensitive, selective, and rapid detection of proteins and DNA are important tools in bioanalytical chemistry. The combination of electrochemistry and metal-based nanoparticles (metal nanoparticles and quantum dots) serving as electrochemically active labels provides an elegant way to detect DNA and proteins [1-3]. The principle of the detection scheme is to label the target biomolecules with the selected nanoparticles and to convert the labelling nanoparticles to the respective free metal cations which are detected by electrochemical stripping analysis. Gold nanoparticles are the most common labels used in electrochemical detection of proteins and DNA. However, the voltammetric detection of Au(III) (normally performed at carbon-based electrodes) lacks in sensitivity while labelling with gold nanoparticles does not allow multiple detection of more than one biomolecules in a single assay. Quantum dots (nanocrystals composed of metal salts) offer an attractive alternative as electrochemical labels with greater versatility since they allow higher detection sensitivity (by selecting a proper combination of the electrode material and composition of nanocrystals) and the possibility to perform multi-analyte assays in a single run.

In this work, various examples are described for the electrochemical assay of biomolecules using nanoparticles labels. The application of different fabrication technologies (thin-film deposition, screen-printing, injection-molding) is demonstrated for the construction of electrochemical sensors for the sensitive detection of DNA and proteins.

References

[1] L. Ding, A.M. Bond, J. Zhai, J. Zhang, Anal. Chim. Acta, 797 (2013) 1.
[2] C. Kokkinos, A. Economou, Anal. Chim. Acta, 961 (2017) 12.
[3] E. Valera, A. Hernandez-Albors, M.P. Marco, TrAC Trends Anal. Chem., 79 (2016) 9.

T2
Food security: Innovative approaches based on apta-sensors and apta-assays for the detection of mycotoxins

Jean Louis Marty*

Sensbiotech, Université de Perpignan, Via Domitia Via Domitia, 52 Avenue Paul Alduy, Perpignan CEDEX 66860, France
**Corresponding author: sensbiotech@gmail.com and jlmarty@univ-perp.fr*

The analysis of foods to assess the presence of chemical contaminants is a practice of crucial importance for ensuring food safety and quality. Over the past decade, the control of food safety has been mainly carried out through product testing rather than process control. Chemical contaminants can be present in foods and feed mainly as result of the use of agrochemicals, such as residues of pesticides and veterinary drug contamination from environmental sources (water, air and soil pollution), cross contamination or formation during the food processing, migration from food packaging materials, presence or contamination of natural toxins.

Natural toxins are defined as poisonous substances, which are synthesized by various organisms as animals, certain plant species or by microorganisms. Due to their ubiquitous occurrence and the wide range of chemical structure of produced toxins, they represent an important economic and health risk.

Among them, mycotoxins are toxic metabolites produced by fungi, mostly by saprophytic moulds on different foodstuffs. Additionally, they are also present in many plant pathogens. They have harmful effect on human and animal health. Mycotoxins are considered as harmful naturally occurring secondary metabolites. Mycotoxin contamination has attracted the worldwide attention and has been considered as major financial problem due to the huge economic loses mainly based on human health, animal productivity, and national and international level trade there must be a proper legislation to set the acceptable limit of toxins for the purpose to minimize the exposure to mycotoxins. This kind of legislation will help in taking action against the improper usage of chemicals in agriculture sector, storage of products such as wheat, rice and other crops, and proper control of those products is required in future to ensure health impact of human beings and animals

The classical techniques have some drawbacks such as high cost and less sensitivity etc. In order to address these issues, various methods have been developed. Among these, biosensors are considered as promising tool in the assessment of mycotoxin food contamination. Electrochemical and optical aptasensors are promising methods. They offer the advantages of low cost, low power consumption, and high stability. This presentation mainly focuses on the methods development in the sense that how mycotoxins can be detected from new emerging bio-analytical approaches. Several applications of determination of mycotoxins in food and feed will be discussed.

T3
Electrochemical impedance spectroscopy: fundamentals and applications to sensors and biosensors

Christopher M.A. Brett*

Department of Chemistry, CEMMPRE, Faculty of Sciences and Technology, University of Coimbra, 3004-535 Coimbra, Portugal
**Corresponding author: cbrett@ci.uc.pt*

The fundamentals of electrochemical impedance spectroscopy relevant to characterizing electrode-solution interfaces and modifier films on electrode surfaces will be outlined. The electrical equivalents of different elements in sensor and biosensor platforms will be discussed, and how combinations of resistances and capacitances lead to an electrical equivalent circuit that models the frequency-dependent impedance. The more appropriate representations of impedance spectra for evaluation of sensor and biosensor platforms will be shown; the necessity of a physical model of the electrode or modified electrode-solution interface that can be understood will be emphasized. Two ways of carrying out impedance experiments with and without redox probes in solution and the information that they can furnish will be examined, and the advantages of each approach will be discussed. Illustrative examples from the analysis of impedance spectra in the characterisation of the build-up and application of sensor and biosensor platforms will be given. Perspectives for quantitative impedimetric sensing will be indicated.

References

[1] C.M.A. Brett, ECS Transactions, 13(13) (2008) 67-80.
[2] C.M.A. Brett, Molecules, 27 (2022) 1497.

T4
Employing acoustic wave biosensors for applications in healthcare and agro/food safety

Electra Gizeli*

Department of Biology, University of Crete, Vassilika Vouton, Heraklion, 70013, Greece
Institute of Molecular Biology and Biotechnology-FORTH, 100 N. Plastira Str., Heraklion 70013, Greece
** Corresponding author: gizeli@imbb.forth.gr*

Acoustic wave devices are used as sensitive biosensors for the detection of a wide range of substances and in several areas, e.g., healthcare, environmental monitoring and food/plant-safety. Commonly used acoustic devices are the Quartz Crystal Microbalance (QCM) normally together with dissipation monitoring (QCM-D) for higher detection-flexibility and the surface acoustic wave (SAW) device, combined with a waveguide layer for enhanced sensitivity (Love wave geometry). SAW devices are also available in a single, dual or array format and can be integrated with microfluidics in a lab-on-chip platform.

This lecture will give an overview of sensing principles and applications of the above two types of acoustic wave biosensors explaining the physics, mechanical and fabrication challenges for integrated acoustic platforms, surface functionalization issues, sample pre-treatment and finally detection and validation using real samples. Examples will be given within two areas: healthcare during the detection of circulating tumor DNA within the context of liquid biopsy [1] and agro/food safety during the testing of milk samples for the presence of pathogens such as *Salmonella* [2].

References

[1] N. Naoumi, et al., Acoustic array biochip combined with allele-specific PCR for multiple cancer mutation analysis in tissue and liquid biopsy. ACS Sensors, 7 (2022) 495-503. https://doi.org/10.1021/acssensors.1c02245.

[2] G. Papadakis, et al. Micro-nano-bio acoustic system for the detection of foodborne pathogens in real samples. Biosens. Bioelectron., 111 (2018) 52-58. https://doi.org/10.1016/j.bios.2018.03.056.

T5
Antifouling surface chemistry on acoustic wave devices

Michael Thompson*, Aries Delica, Brian De La Franier

Department of Chemistry, University of Toronto, 80 St. George St., Toronto, Ontario M5S 3H6, Canada
** Corresponding author: m.thompson@utoronto.ca*

Non-specific adsorption (NSA) or fouling of sensor surfaces has constituted a major problem for operation of such devices in difficult media for many years. This is especially the case for application in biological fluids, and food products such as milk, which contain a high concertation of protein and other moieties. In recent years, we have shown that a high frequency acoustic wave device (EMPAS), which involves a silica substrate, can be surface-modified with an ultra-thin covalently-attached monolayer in order to dramatically reduce NSA [1]. The chemistry is based on a monoethylene glycol, which contains both distal -OH and intra-chain glycol groups (short form, MEG-OH). Interfacial analysis by neutron reflectometry and MD calculations [2,3] strongly suggest that the antifouling property is associated with an interstitial zone of liquid crystalline water.

Equivalent thiol-based surface chemistry on gold, which is often employed as an electrode material on TSM acoustic devices, does not display the same antifouling properties [4,5]. This is attributed to the prevention of interstitial hydration because of close-packing of the SAM. To investigate this argument further we synthetized a dithiol species, $(SH)_2$-MEG-COOH, for Au modification which was considered to allow the afore-mentioned layer of hydration. The antifouling character of this chemistry against a 20% solution of goat serum was studied via a standard TSM configuration. The results of these experiments showed that a significant reduction in NSA was observed, although not as dramatic as the case with the Si surface of the EMPAS system. However, the finding does confirm that the formation of interstitial water in an SAM is critical in terms of the reduction of NSA. This is potentially a very important consideration when designing surface chemistries for application of acoustic wave sensors in the type of samples mentioned above. We are proceeding to explore further surface-modifying species that maybe capable of enhanced antifouling properties on gold.

Acknowledgment: This research was supported by the Natural Sciences and Engineering Research Council of Canada (NSERC).

References

[1] J.C-C. Sheng, B. De La Franier, M. Thompson, Materials, 14 (2021) 472-487.
[2] N.M. Pawlowska, H. Fritzsche, M. Vezvaiem, C. Blaszykowski, S. Sheikh, M. Thompson, Langmuir, 30 (2014) 1199-1203.
[3] S. Sheikh, C. Blaszykowski, D. Thompson, M. Thompson, J. Coll. Interface Sci., 437 (2015) 197-204.
[4] B. De La Franier, M. Thompson, Materials, 14 (2021) 4158-4166.
[5] A. Delica, "Exploring Spacing Effects in Antifouling Monoethylene-Glycol Layers on Gold-Quartz Biosensors", University of Toronto, Undergraduate CHM 499 Thesis, 2022.

T6
From the detection of an acoustic signature of event to impactful applications

Ilia N. Ivanov*

Center for Nanophase Materials Science. Oak Ridge National laboratory, Oak Ridge, Tennessee, 37831 USA
** Corresponding author: ivanovin@ornl.gov*

Acoustic detection of an interfacial events evolved over last years to become excellent addition to the toolbox of analytical techniques now commonly used in the laboratory. Automation of liquid delivery, the development of a multi acoustic sensor platforms and automation of data processing opened new opportunity to broaden the range of scientific questions we can address using acoustic sensor technology.

Acoustic technique becomes especially powerful when it complemented by other analytical techniques, including electrochemical, optical. The design of experiment where multiple complementary techniques are used created a new research paradigm for researcher to address advanced scientific challenges [1-3].

We will look at several examples of multimodal characterization of materials and discuss possible application of acoustic technique for advanced polymer characterization, development of carbon dioxide reduction technology and polymer upcycling.

References

[1] US Patent 17/483,226 “Multimodal dynamic characterization of materials under programmable environment and environment prediction”.

[2] L.A. Galuska, E.S. Muckley, Y. Cao, et al. SMART transfer method to directly compare the mechanical response of water-supported and free-standing ultrathin polymeric films. Nat. Commun., 12 (2021) 2347. https://doi.org/10.1038/s41467-021-22473

[3] E.S. Muckley, L. Collins, B.R. Srijanto, I.N. Ivanov, Machine learning-enabled correlation and modeling of multimodal response of thin film to environment on macro and nanoscale using “Lab-on-a-Crystal.” Adv. Funct. Mater., 30 (2020) 1908010. https://doi.org/10.1002/adfm.201908010

T7
Micromotors go *in-vivo*: From test tubes to live animals

Joseph Wang*

Department of Nanoengineering, University of California San Diego, La Jolla, California, 92093, United States
**Corresponding author: josephwang@ucsd.edu*

Nanoscale robots that can effectively convert diverse energy sources into movement and forces represent a rapidly emerging and fascinating robotic research area. Such nanoscale robots offer impressive capabilities, including greatly enhanced power and cargo-towing forces, multi-functionality, easy surface functionalization, and versatility. The new capabilities of modern nanorobots indicate immense potential for a variety of biomedical applications, and should have major impact on disease diagnosis, treatment, and prevention. Recent *in vivo* applications using different types of biocompatible and biodegradable microrobots will be illustrated, including enhanced drug delivery towards enhanced treatment of stomach bacterial infection, active vaccine delivery, autonomous gastric fluid neutralization, the ability to selectively localize at desirable segments of the GI tract, or efficient intracellular delivery of functional proteins and nucleic acids.

Workshop
„Biosensors in food safety“

Abstracts of Invited Lectures

IL1
Specific nanobodies for accurate detection of food contaminants

Feng Wang[1,2*], Hong Wang[2], Bruce D. Hammock[3]

[1] College of Light Industry and Food Technology, Zhongkai University of Agriculture and Engineering, Guangzhou 510225, China;
[2] College of Food Science, South China Agricultural University, Guangzhou 510642, China;
[3] Department of Entomology and Nematology and UCD Comprehensive Cancer Center, University of California, Davis, California 95616, United States
** Corresponding author: wangfeng_sp@163.com*

Immunology-based assays have been widely used in detection of some pollutants in foods. The reported studies were mostly based on polyclonal antibodies (pAbs) and monoclonal antibodies (mAbs), which also had shortcomings in terms of thermal stability and resistance to organic solvents. In contrast to the traditional pAbs and mAbs, nanobodies are ~15 kDa protein fragments derived from camelid heavy chain antibodies with superior performance. The specific nanobodies are new kind of biorecognition elements empowered by phage display technology, yeast surface display technology, and other innovative methods with stringent biopanning strategies. In parallel, recent progress in nanobody-based immunoassays are increasingly reported for specific and sensitive detection of toxic pollutants in foods, such as small molecule compounds, foodborne pathogens, and food allergens. They could exhibit superior performance in the enhancement of assay sensitivity, the high stability of thermal treatment, and the tolerance of organic solvent. In conclusion, nanobodies could serve as unique antibodies for the accurate immunodetection of various contaminants in food since the convenient strategy for nanobody generation.

References

[1] R. Peltomaa, R. Barderas, E. Benito-Peña, et al. Anal. Bioanal. Chem., 414 (2022) 193-217.
[2] S. Muyldermans, Ann. Rev. Biochem., 82 (2013) 775-797.
[3] C.S. Bever, J.X. Dong, N. Vasylieva, et al. Anal. Bioanal. Chem. 408 (2016) 5985-6002.
[4] Y. Wang, Z. Fan, L. Shao, et al. Int. J. Nanomedicine, 11 (2016) 3287.
[5] M. Yamagata, J.R. Sanes, Proc. Natl. Acad. Sci., 115 (2018) 2126-2131.
[6] Y. Wang, Y. Xianyu, Small Methods, (2022) 2101576.
[7] C. McMahon, A.S. Baier, R. Pascolutti, et al. Nature Struct. Molec. Biol., 25 (2018) 289-296.
[8] F. Wang, Z.F. Li, Y.Y. Yang, et al. Anal. Chem., 92 (2020) 11935-11942.
[9] F. Wang, Y.Y. Yang, D.B. Wan, et al. Food Control, 136 (2022) 108835.

IL2
Peptides functionalized conducting polymer-graphene OFETs for detection of aqueous phase pollutants

Mahendra Shirsat*

Department of Physics, RUSA Centre for Advanced Sensor Technology, Dr. Babasaheb Ambedkar Marathwada University, Aurangabad – 431001 (MS) India
** Corresponding author: mdshirsat.phy@bamu.ac.in*

The major sources of water contamination are heavy metal ions which are being released in the environment through anthropogenic and natural sources such as electroplating, mining, smelting, battery manufacturing, textile printing and the weathering of minerals, erosion, volcanic activities etc. The common heavy metal contaminants include arsenic (As), lead (Pb), mercury (Hg), cadmium (Cd) and chromium (Cr). Heavy metals are inorganic pollutants which pose a serious threat to human and environmental safety, and their effective removal is becoming an increasingly urgent issue. Most of these metal ions are highly toxic, nonbiodegradable and bioaccumulative. Therefore, detection/removing of these heavy metals are crucial in the current situation. There are several techniques based on spectrometric, fluorescent, electrochemical, colorimetric, and optical methods that have been reported to date. However, it has certain drawbacks, e.g., low-cost, easy-to-use, tedious sample preparation, pre-concentration procedures, expensive instruments, professional personnel, and reliable device fabrication are not possible. However, the field effect transistor (FET) based heavy metal ions sensors possesses low-cost fabrication, good sensitivity, mechanical flexibility, portability, and biocompatibility. The scientific community recently exploring various materials for the detection of heavy metal ions from aqueous media with the help FET modality using various materials viz. organic conducting polymers (OCPs) [1], carbon nanotubes (CNTs), graphene [2], bioreceptors [3], metal nanoparticles [4] etc. However, some polymeric materials (e.g., P3HT and PBTTT) are not stable in the water medium and degrade almost immediately [5,6]. Therefore, alternative organic-conducting polymer material needs to be explored for the sensing application, which can be efficiently performed under liquid medium for the electrical detection of heavy-metal ions. Among the conducting polymers, the commercially available PEDOT:PSS has proven its stability in an aqueous environment and possesses excellent potential applications in FET due to its low cost, high transparency, and excellent processability [7–10]. In the present investigation deals with the synthesis and characterization of the graphene and organic conducting polymers (viz. 5,5–bis–(7dodecyl-9H-fluoren-2-yl)-2,2-biothiophene (DDFTTF); poly(3,4-thylenedioxythiophene) poly(styrenesulfonate) (PEDOT: PSS), and poly(isoindigo–bithiophene) (PII2T)) etc.) composite. The composite of graphene/OCPs will be deposited on interdigitated electrodes by dip coating/drop cast/spin coating/electrochemical technique and morphological, spectroscopic, structural and electrical characterization will be carried out. Further, the composite of graphene/OCPs will be modified with peptides to inculcate selectivity. The fabricated sensor was tested with back gated FET to detect various heavy metal ions.

References

[1] M.A. Deshmukh, G.A. Bodkhe, S. Shirsat, A. Ramanavicius, M.D. Shirsat, Nanocomposite platform based on EDTA modified Ppy/SWNTs for the sensing of Pb (II) ions by electrochemical method, Front. Chem., 6 (2018) 451.

[2] T. Al-Gahouari, G. Bodkhe, P. Sayyad, N. Ingle, M. Mahadik, S.M. Shirsat, M. Deshmukh, N. Musahwar, M. Shirsat, Electrochemical Sensor: L-cysteine induced selectivity enhancement of electrochemically reduced graphene oxide–multiwalled carbon nanotubes hybrid for detection of lead (Pb^{2+}) ions, Front. Mater., 7 (2020) 68.

[3] M. Mahadik, H. Patil, G. Bodkhe, N. Ingle, P. Sayyad, T. Al-Gahaouri, S. Shirsat, M.D. Shirsat, EDTA modified PANI/GO composite based detection of Hg (II) ions, Front. Mater., 7 (2020) 81.

[4] L. Zhu, L. Xu, B. Huang, N. Jia, L. Tan, S. Yao, Simultaneous determination of Cd (II) and Pb (II) using square wave anodic stripping voltammetry at a gold nanoparticle-graphene-cysteine composite modified bismuth film electrode, Electrochimica Acta., 115 (2014) 471–477.

[5] O. Knopfmacher, M.L. Hammock, A.L. Appleton, G. Schwartz, J. Mei, T. Lei, J. Pei, Z. Bao, Highly stable organic polymer field-effect transistor sensor for selective detection in the marine environment, Nat. Commun., 5 (2014) 2954. https://doi.org/10.1038/ncomms3954.
[6] B.L. Rivas, B.F. Urbano, J. Sánchez, Water-soluble and insoluble polymers, nanoparticles, nanocomposites and hybrids with ability to remove hazardous inorganic pollutants in water, Front. Chem., 6 (2018) 320.
[7] D.A. Bernards, G.G. Malliaras, Steady-state and transient behavior of organic electrochemical transistors, Adv. Funct. Mater., 17 (2007) 3538–3544.
[8] S.H. Kim, J. Kim, S. Nam, H.S. Lee, S.W. Lee, J. Jang, Tuning the work function of printed polymer electrodes by introducing a fluorinated polymer to enhance the operational stability in bottom-contact organic field-effect transistors, ACS Appl. Mater. Interfaces., 9 (2017) 12637–12646.
[9] L. Contat-Rodrigo, C. Pérez-Fuster, J.V. Lidón-Roger, A. Bonfiglio, E. García-Breijo, Characterization of screen-printed organic electrochemical transistors to detect cations of different sizes, Sensors, 16 (2016) 1599.
[10] J.T. Mabeck, G.G. Malliaras, Chemical and biological sensors based on organic thin-film transistors, Anal. Bioanal. Chem., 384 (2006) 343–353.

IL3
Applications of optical immunosensors to food safety

Panagiota Petrou*

Immunoassays/Immunosensors Lab, Institute of Nuclear & Radiological Sciences & Technology, Energy & Safety, NCSR "Demokritos", 15341 Aghia Paraskevi, Greece
** Corresponding author: ypetrou@rrp.demokritos.gr*

Optical biosensors are one of the most widely used category of sensing tools due to their high detection sensitivity, immunity to parasitic electronic noise, multi-analyte capabilities and in many cases ability for label-free detection of biomolecular interactions. Amongst label-free optical sensors, those relying on silicon photonics are especially promising for development of small size devises appropriate for applications at the point-of-need, once the hybrid integration of light sources and detectors is realized in a cost and labor effective way. In this context, our work the last 10 years focuses on the development of label-free optical immunosensors based either on refractrometric or reflectrometric transduction principles. The refractrometric sensors were based on silicon photonic chips that combine all optical components, both active and passive, onto the same substrate. The transducers are silicon nitride waveguides shaped as Mach-Zehnder interferometers (MZI) to enable label-free monitoring of binding reactions. In addition, the implementation of white light emitting diodes as light sources instead of monochomatic ones as in standard MZIs lead to a new sensing approach, the broadband Mach-Zehnder interferometry, which provided for higher detection sensitivity since it uses the whole white light spectrum to detect changes in refractive index due to binding reactions [1]. The approach followed for the monolithic integration of arrays of thin silicon nitride optical waveguides, light emitting diodes and photodetectors on a single silicon chip as well as the different silicon photonic sensors realized over the years will be presented. The chips were transformed to immunosensors through chemical activation and biological functionalization with specific recognition biomolecules [2]. These methods have been optimized combining data from model assays run with the chips and surface analysis and characterization methods. Regarding reflectrometric sensors, they were also realized on silicon chips with an appropriate dielectric layer on top and using a broadband light source thus leading to a new sensing concept referred as White Light Reflectance Spectroscopy (WLRS) [3]. The two label-free sensing approaches have been employed as immunosensors for the determination of single or panels of analytes related to food safety. The analytes determined included allergens, mycotoxins, pesticides, and bacteria in several food matrices (milk, cheese, beers, water, wine, etc.) [2, 3]. The analytical characteristics of the assays developed with the different sensor formats will be discussed in comparison to those reported in literature for other optical sensors.

References

[1] K. Misiakos, I. Raptis, E. Makarona, A. Botsialas, A. Salapatas, P. Oikonomou, A. Psarouli, P.S. Petrou, S.E. Kakabakos, K. Tukkiniemi, M. Sopanen, G. Jobst, Opt. Exp., 22 (2014) 26803-26813.

[2] M. Angelopoulou, P.S. Petrou, E. Makarona, W. Haasnoot, I. Moser, G. Jobst, D. Goustouridis, M. Lees, K. Kalatzi, I. Raptis, K. Misiakos, S.E. Kakabakos, Anal. Chem., 90 (2018) 9559−9567.

[3] V. Anastasiadis, G. Koukouvinos, P.S. Petrou, A. Economou, J. Dekker, M. Harjanne, P. Heimala, D. Goustouridis, I. Raptis, S.E. Kakabakos, Biosens. Bioelectron., 153 (2020) 112035.

IL4
Electrochemical sensing of glycoproteins at charged surfaces.

Veronika Ostatná*, Hana Černocká, Mojmír Trefulka, Ludmila Římánková, Tatiana Galicová

Institute of Biophysics, The Czech Academy of Sciences, v.v.i., Královopolská 135, 61265 Brno, Czech Republic
** Corresponding author: ostatna@ibp.cz*

For many years, the sugars were considered only as nutritional source. However, their role appears more complex. Sugars play essential role in many cellular mechanisms, such as cell–cell and cell–biomolecule interactions. Free and conjugated milk oligosaccharides display inhibitory activity against broad spectrum of pathogens. In recent years, attention is focused on milk components containing sialic acids increases.

Complexity of glycans together with their similar physicochemical properties complicate progress in glycan analysis [1]. Nowadays, the main approaches for glycan analyses are robust and reliable methods, such as mass spectrometry linked with liquid chromatography or capillary electrophoresis. Nevertheless, these methods require an experienced operator and are highly time and sample-consuming. An alternative way for glycan analyses can be electrochemical methods. They appear useful in analysis of free glycans as well as those bound in glycoproteins [1]. Recently, we showed that the terminal sialic acid presence in glycans stabilizes glycoprotein molecule against effects of electric field. The glycoproteins containing sialic acid behaved differently at charged surfaces that those without sialic acid, what allows to utilize constant current chronopotentiometry for easy determination of sialoglycoproteins [2].

This research was supported by the Czech Science Foundation by project No.22-26590S.

References

[1] E. Paleček, J. Tkáč, M. Bartošík, T. Bertók, V. Ostatná, J. Paleček, Chem. Rev., 115 (2015) 2045–2108.
[2] H. Černocká, L. Římánková, V. Ostatná, J. Electroanal. Chem., 902 (2021) 115801.

IL5
Electrochemical aptasensors developed for detection of biointeractions

Arzum Erdem*

Analytical Chemistry Department, Faculty of Pharmacy, Ege University, Bornova, 35100, Izmir, Turkey

** Corresponding author: arzum.erdem@ege.edu.tr*

Electrochemical biosensors are coupling the characteristic specificity of biorecognition reactions with high sensitivity of physical transducers that exhibit a great potential for clinical, environmental, or forensic applications.

Aptamers are synthetic nucleic acid sequences that could selectively bind to their target molecules. The synthesis and selection of aptamers are performed by SELEX (Systematic Evolution of Ligands by Exponential enrichment) method. Aptamer based biosensors are defined as aptasensors, which can be applied for detection of proteins, toxins or drugs. An overview to electrochemical aptasensors developed for monitoring of different biointeractions has been introduced in the present study with their advantages and further applications.

Workshop
„Biosensors in food safety“

Abstracts of Short Communications

SC1
Low-cost, AChE-based, electrochemical sensors for pesticide detection in vegetable oils: sensor fabrication methodology and measurement matrix effects on sensor performance

Dimitra Tsounidi[1], Dionysis Soulis[1], Nikitas Melios[1,2], Chrysoula Chandrinou[3], Ioanna Zergioti[3], George Tsekenis[1]*

[1] *Biomedical Research Foundation of the Academy of Athens, Soranou Ephessiou 4, 11527 Athens, Greece*
[2]*Department of Chemistry, National and Kapodistrian University of Athens, Panepistimiopolis, Athens 15771, Greece*
[3]*School of Mathematical and Physical Sciences, Physics Department, National Technical University of Athens, Heroon Polytechneiou 9, 15780 Athens, Greece*
** Corresponding author: gtsekenis@bioacademy.gr*

Despite the fact that a considerable amount of effort has been invested in the development of biosensors for the detection of pesticides, there is still a lack of a simple and low-cost platform that can reliably and sensitively detect their presence in real samples. Herein, an enzyme-based biosensor for the determination of both carbamate and organophosphorus pesticides is presented that is based on acetylcholinesterase (AChE) immobilized on commercially available screen-printed carbon electrodes (SPEs) modified with carbon black (CB), as a means to enhance their conductivity. Most interestingly, two different methodologies to deposit the enzyme onto the sensor surfaces were followed with strikingly different results obtained depending on the family of pesticides under investigation. Furthermore, and towards the uniform application of the functionalization layer onto the SPEs' surfaces, the laser induced forward transfer (LIFT) technique was employed in conjunction with CB functionalization, which allowed a considerable improvement of the sensor's performance to be attained. Under the optimized conditions, the fabricated sensors (Figure 1) allowed the detection of both pesticides in buffer as well as appropriately-pretreated oil samples at concentrations below 10 ppb, which is the maximum residue limit permitted by the European Food Safety Authority [1]. In addition, the contribution of the extracted matrix to AChE inhibition and thus on the performance of the sensors was also evaluated, through the interrogation of the sensors with different vegetable oil samples (olive oil, sunflower oil) of different geographical and varietal origins.

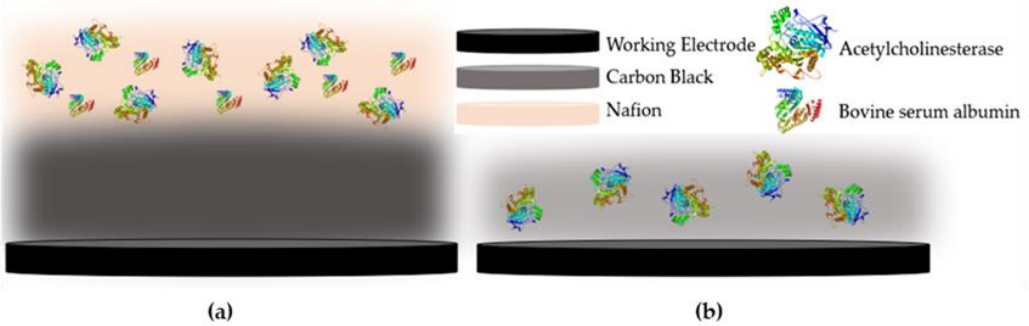

Figure 1. Graphical representation of the fabricated enzyme-based biosensor using two different approaches for enzyme immobilization onto the SPE surfaces

References

[1] D. Soulis, M. Trigazi, G. Tsekenis, C. Chandrinou, A. Klinakis, I. Zergioti, Molecules, 25 (2020) 4988.

SC2
Detection of cadmium in aqueous medium by electrochemical method

Kiran S. Sontakke, Vijaykiran N. Narwade, Mahendra D. Shirsat*

RUSA Centre for Advance Sensor Technology, Department of Physics, Dr. Babasaheb Ambedkar Marathwada University, Aurangabad, Maharashtra, India.

**Corresponding author: mdshirsat.phy@bamu.ac.in*

Cadmium (Cd) is a toxic heavy metal and represents health risk for both humans and animals. It is naturally occurring pollutant in the environment that is derived from agriculture and industrial sources. Other sources of Cd primarily occur through the ingestion of contaminated food and water, plastics and nickel-cadmium battery. Cd accumulates in plants and animals for long years. Epidemiological data suggest that occupational and environmental Cd exposure may be related to various types of cancer, including, breast, lung, prostate, nasopharynx, pancreas, and kidney. It has been also demonstrated that environmental Cd may be a risk factor for osteoporosis. The liver and kidneys are extremely sensitive to Cd' toxic effects [1]. The World Health Organization (WHO) has set the allowable level of Cd in drinking water at 27 nM (0.003 mg/L). The EPA recommends 1 μg/kg/day and 0.5 μg /kg/day as reference doses for human exposure to Cd^{2+} in food and water. However, Cd concentrations released into water from industrial activities are much higher than the prescribed limits, causing environmental contamination and increasing hazards to human health [2].

The mechanisms of electrochemical sensors must be understood in order to increase the assay performance such as selectivity, sensitivity, detection limit, repeatability, and reproducibility for application scenarios. We developed a Cd(II) electrochemical sensor based on the composite of LGSH@PEDOT:PSS/MWCNTs-COOH that exhibited a sensitivity of 10.69 μA/ppm and a detection limit of 1 ppm. Moreover, the sensor exhibited good selectivity, repeatability (RSD=1.85%), and reproducibility (RSD = 4.73%). This favorable result makes the investigated surface composite very promising for the developed of the next generation electrochemical sensing.

References

[1] G. Genchi, M.S. Sinicropi, G. Lauria, A. Carocci, A. Catalano, Int. J. Environ. Res. Public Health, 17 (2020) 3782.

[2] G. Zhang, S. Hu and X. Jia, Front. Bioeng. Biotechnol., (2021) https://doi.org/10.3389/fbioe.2021.799781.

SC3
Surface plasmon resonance biosensor for detection of tramadol in drinking water

Magdalena Čapková, Erika Hemmerová, Jiří Homola*

Institute of Photonics and Electronics, The Czech Academy of Sciences, Chaberská 57, 182 51 Prague, Czech Republic
**Corresponding author: homola@ufe.cz*

The quality of drinking water plays an important role in the public health protection. Apart from microbial contamination, chemical contamination with pesticides, pharmaceutical drugs and various other substances may also represent serious health risk. In order to prevent serious health consequences, the presence of such chemicals in the drinking water needs to be monitored. This requires development of the new analytical methods that are sensitive, selective and affordable and enable in situ analysis.

In this work we present the first reported use of a surface plasmon resonance (SPR) biosensor for detection of pharmaceutical drug tramadol in drinking water. The developed assay utilizes the inhibition detection format combined with signal enhancement via functionalized gold nanoparticles (Figure 1). This assay is fast (time of analysis ~ 45 min) and requires minimal sample volume (~ 1 ml) and preparation (filtration, addition of buffer). The limit of detection was determined as 2.9 nM. In order to demonstrate the applicability of the developed assay for the real sample analysis, a sample of tap water from public water distribution network in Prague was analyzed.

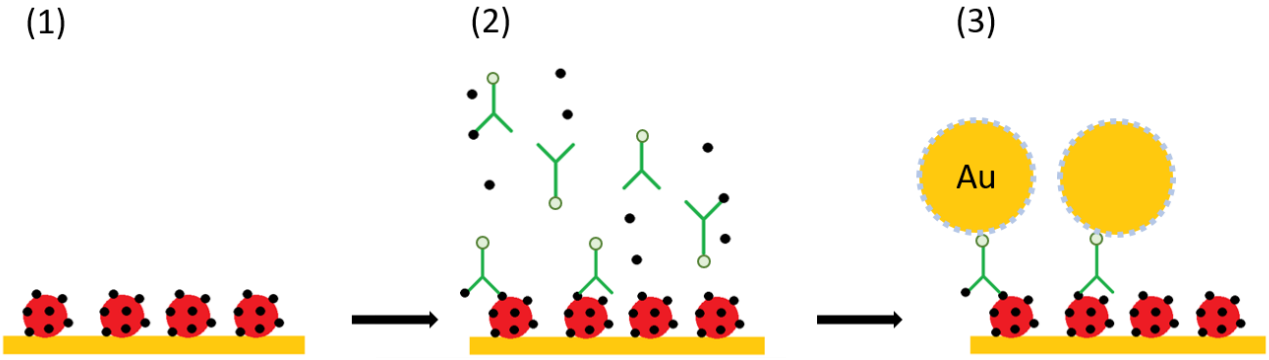

Figure 1. Schematic representation of the assay for detection of tramadol: (1) surface of the SPR chip functionalized with the analogue of the tramadol. (2) incubation of the sample with the antibody against tramadol and capture of the unreacted antibody. (3) enhancement of the sensor response via functionalized gold nanoparticles.

SC4
Galectin-1 binding to model lipid membrane investigated by the combination of QCM-D and fluorescence methods

Federica Scollo[1*], Gabriele Nicita[2], Anna-Kristin Ludwig[3], Herbert Kaltner[3], Hans-Joachim Gabius[3], Peter Kapusta[1], Giuseppe Maccarrone[2], Martin Hof[1].

[1]Biophysical Chemistry, J.H. Institute of Physical Chemistry, Prague, Czech Republic;
[2]Department of Chemical Sciences, University of Catania, Catania, Italy;
[3]Faculty of Veterinary Medicine, Institute of Physiological Chemistry, Ludwig-Maximilians-University, Munich, Germany
**Corresponding author: federica.scollo@jh-inst.cas.cz*

Galectins are a ubiquitous family of galactose-binding proteins, involved in a variety of functions, spanning from RNA splicing to cell growth regulation, including cell adhesion, embryogenesis, inflammation and immune function, apoptosis, angiogenesis and tumor metastasis. Nowadays, fourteen human galectins are known, commonly grouped into three different types, according to their different architecture. However, all of them have a common feature: they possess one or more β-sandwich carbohydrate recognition domain/s (CRD/s) by which they interact with molecules having a galactoside moiety. Still, the reason why in nature galectins exist in different forms has not yet been clarified. Among all of them, galectin-1 is one of the most important, being implicated in T-cells communication. It is believed to express its function by binding specifically the monosialotetrahexosylganglioside (GM1). This binding has been only hypothesized and previously indirectly showed, either employing too sophisticated or non-physiologically relevant systems, such as neuroblastoma cells or glycodendrimers [1,2]. Therefore, we believe that a clear direct proof is still currently missing. In this work, we investigate the interaction of galectin-1 with different types of physiologically relevant model membranes containing GM1, by using a combination of different techniques. Specifically, we employed both fluorescence-based, i.e. Förster Resonance Energy Transfer and confocal Microscopy combined with Quartz Crystal Microbalance with Dissipation Monitoring, a highly sensitive and label-free technique. To the best of our knowledge, our data demonstrate for the first time that galectin-1 is interacting with model membranes and suggest a specific interaction with GM1.

References

[1] J. Kopitz, C. von Reitzenstein, M. Burchert, M. Cantz, H.J. Gabius, Galectin-1 is a major receptor for ganglioside GM1, a product of the growth-controlling activity of a cell surface ganglioside sialidase, on human neuroblastoma cells in culture. J. Biol. Chem., 273 (1998) 11205-11211.

[2] S. Zhang, R.O. Moussodia, C. Murzeau, H.J. Sun, M.L. Klein, S. Vertesy, S. Andre, R. Roy, H.J. Gabius, V. Percec, Dissecting molecular aspects of cell interactions using glycodendrimersomes with programmable glycan presentation and engineered human lectins. Ang. Chemie, 127 (2015) 4108-4112.

SC5
Application of electrochemical biosensors and DNA aptamers for the detection of pathogenic bacteria

Veronika Oravczová[1*], Judit Süle[2], Tibor Hianik[1]

[1]*Faculty of Mathematics, Physics, and Informatics, University of Comenius, Mlynská Dolina 842 48 Bratislava 4, Slovakia*
[2]*Hungarian Dairy Research Institute Ltd., Lucsony utca 24. 9200 Mosonmagyarovar, Hungary*
**Corresponding author: oravczova2@uniba.sk*

According to World Health Organization (WHO), approximately 600 million people get sick from contaminated food, out of which 420 000 die each year worldwide [1]. Therefore, early detection of foodborne pathogens is of utmost importance for the prevention of diseases. Traditional methods of detection bacteria are rather laborious and require up to 72 hours to confirm a negative result and up to a week to confirm positive contamination of food [2]. Rapid methods available for commercial use are based on either polymerase chain reaction (PCR) or immunoassays, which are usually costly and require trained personnel [3]. We report the development of an electrochemical biosensor based on DNA aptamers for the detection of pathogenic bacteria *Listeria monocytogenes*. The working surface of the gold electrode was functionalized with DNA aptamers specific to *Listeria monocytogenes* using the carbodiimide method. Using electrochemical impedance spectroscopy (EIS) and differential pulse voltammetry (DPV) we have found that following incubation of the sensing surface with various concentrations of bacteria an increase of the current measured by DPV at presence of the redox mediator methylene blue (MB) occurred. This is due to the adsorption of the positively charged MB to the negatively charged bacteria at the sensor surface. EIS at presence of redox couple Fe^{-3}/Fe^{-4} revealed increase of the charge transfer resistance following elevated concentrations of bacteria. The specificity of detection was confirmed using *Escherichia coli* and *Listeria innocua*, as a negative control. The developed aptasensor showed promising sensitivity and specificity for real-time detection of *Listeria monocytogenes*. The limit of detection was estimated as 400 CFU (colony forming units)/ml with a detection time of 20 minutes.

Acknowledgments: This work was funded under European Union's Horizon 2020 research and innovation program through the Marie Skłodowska-Curie grant agreement No 101007299 as well as by Science Grant Agency VEGA, project No. 1/0419/20.

References

[1] WHO, 2020. World Health Organization. https://www.who.int/activities/estimating-the-burden-of-foodborne-diseases.
[2] P. Mandal, A.K. Biswas, K. Choi, U.K. Pal, Food Technol., 6 (2011) 87-102.
[3] J.-F. Law, N.-S. Ab Mutalib, K.-G. Chan, L.-H. Lee, Front. Microbiol., 5 (2015) 770.

SC6
Aptamer-modified gold nanoparticles in colorimetric detection of *E. coli*

Ivan Piovarči*[1], Judit Süle[2], Mihailia Angelopoulou[3], Panagiota Petrou[3], Leda Bousiakou[4], Sotirios E. Kakabakos[3], Tibor Hianik[1]

[1]Faculty of Mathematics, Physics, and Informatics, University of Comenius, Mlynská Dolina 842 48 Bratislava 4, Slovakia
[2]Hungarian Dairy Research Institute Ltd., Lucsony utca 24. 9200 Mosonmagyarovar, Hungary
[3]National Centre for Scientific Research "Demokritos", Patr. Gregoriou E & 27 Neapoleos Str., 15341 Agia Paraskevi, Greece
[4]IMD Laboratories Co, R&D Section, Lefkippos Technology Park, NCSR Demokritos, Agia Paraskeyi, PO Box 60037, 15130 Athens, Greece
**Corresponding author: piovarci.i@gmail.com*

Bacterial contamination in food is dangerous to the human health. Current methods of detection bacterial contamination are sensitive and specific but take a long time to complete. They are also expensive and need specific training, which cause difficulties for routine testing in food laboratories. In this work we have therefore focused on the development of a colorimetric assay using gold nanoparticles (AuNPs) modified by DNA aptamers. DNA aptamers are short oligonucleotides (15-80 bases) that in a solution fold into 3D structure forming binding site for the target including different epitopes on a bacterial surface, such as lipopolysaccharides or proteins. Aptamers can be immobilized at the surfaces where they serve as receptors for detection of bacteria. For example, thiolated aptamers can be chemisorbed on a gold surface including AuNPs. At the same time AuNPs can serve as a transducer of optical signal since they possess a colorimetric response due to aggregation and modification. We modified AuNPs with DNA aptamers specific to *E. coli*. After interaction of the aptamer modified AuNPs with the bacteria for 40 minutes and after addition to 5 M NaCl we observed differences in spectra for AuNPs interacting and not interacting with bacteria, respectively. The limit of detection of this assay was 1.2×10^4 CFU/mL. The specificity of detection has been confirmed using *Salmonella typhimurium* bacteria as a control.

Acknowledgments: This work was funded under European Union's Horizon 2020 research and innovation program through the Marie Skłodowska-Curie grant agreement No 101007299 as well as by Science Grant Agency VEGA, project No. 1/0419/20.

SC7

Detection of *Escherichia coli* in milk by a piezoelectric aptasensor with an anti-fouling coating

Sandro Spagnolo[1*], Brian De La Franier[2], Katharina Davoudian[2], Tibor Hianik[1], Michael Thompson[2]

[1]*Faculty of Mathematics, Physics and Information, Comenius University, Mlynská dolina F1, 842 48 Bratislava, Slovakia.*

[2]*Department of Chemistry, University of Toronto, 80 St. George Street, Toronto, ON M5S 3H6, Canada.*

**Corresponding author: sandrospagnolo1@gmail.com*

Milk is one of the most produced and consumed food in the world. European Union producing over 160 million tons of milk each year. For milk to be safe for consumption, it must have an acceptably low level of microbial contamination and, above all, be free of harmful bacteria, such as *Escherichia coli* or *Staphylococcus aureus*, which could cause illness to consumers. In European Union, the safe bacterial contamination limit in milk is 10^5 colony forming units/mL (CFU/mL), although the best desirable limit is less than 1.5×10^4 CFU/mL. The bacterial load in milk samples is generally measured using the colony count in the agar culture plates. However, this measurement has the major disadvantage of being slow and somewhat unreliable. The development of a biosensor capable of quantifying the number of bacteria present in milk samples would greatly improve the accuracy and speed of milk safety assessment. In this work, we applied *E. coli*-specific DNA aptamers for the development of a very high frequency electromagnetic piezoelectric acoustic sensor (EMPAS). The DNA aptamers were covalently linked to the crystal surface by means of a linker, MEG-Cl, with antifouling properties to be able to prevent any non-specific adsorption of the milk samples on the EMPAS sensor [1]. In this way, such functionalized surfaces were employed to detect *E. coli* and act as sensors capable of selectively measuring these bacteria in PBS buffer or cow's milk samples up to detection limits of 35 and 8 CFU/mL, respectively [2]. These detection limits are well below the safety limits for commercial dairy products, so this detection system holds great promise for the dairy industry for rapid product safety verification.

Acknowledgments: This work was funded under European Union's Horizon 2020 research and innovation program through the Marie Skłodowska-Curie grant agreement No 101007299 as well as by Science Grant Agency VEGA, project No. 1/0419/20.

References

[1] S. Spagnolo, B. De La Franier, T. Hianik, M. Thompson, Biosensors, 10 (2020) 20.
[2] S. Spagnolo, B. De La Franier, K. Davoudian, T. Hianik, M. Thompson, Sensors, 22 (2022) 1853.

SC8
Electrochemical detection of penicillin G and aflatoxin M1 using redox tagged DNA aptamers

Stefanos Karapetis[1*], Leda Bousiakou[1], Veronika Subjakova[2], Tibor Hianik[2]

[1]*IMD Laboratories Co, R&D Section, Lefkippos Technology Park, NCSR Demokritos PO Box 60037, GR-15130 Agia Paraskeyi, Athens, Greece*
[2]*Faculty of Mathematics, Physics and Informatics, Comenius University,* Mlynska dolina F1, 842 48, *Slovakia,*
** Corresponding author: karapetisteve@outlook.com*

In this work, we report the development of electrochemical biosensors for the detection of Penicillin G (PEN) as well as aflatoxin M1 (AFM1) using DNA aptamers. In the case of PEN detection, the aptamers were modified by a redox probe methylene blue (MB) with the following sequence: MB-5'-GGG TCT GAG GAG TGC GCG GTG CCA GTG-3'-SH [1]. The aptamers were immobilized on a gold surface of working electrode via chemisorption, utilizing the Au-S bond. For the detection of AFM1, three different DNA aptamers were used. The first one was modified by the amino group at the 5' end: NH_2-5'-ACT GCT AGA GAT TTT CCA CAT-3' (Aptamer 1) as described by Nguyen *et al*. [2]. In this case, the aptamer was immobilized on a gold surface covered by fourth generation of poly(amido-amine) dendrimers (PAMAM G4) [3]. DNA aptamers modified at 5' end were also used: Biotin-5'-TTT TTT TTT TTT TTT ACT GCT AGA GAT TTT CCA CAT-3' (Aptamer 2) or Biotin-5'-GTT GGG CAC GTG TTG TCT CTC TGT GTC TCG TGC CCT TCG CTA GGC CCA CA-3' (Aptamer 3) [4,5]. The biotinylated aptamers were immobilized on a gold surface covered by neutravidin modified by redox probe ferrocene (Fc). The detection of PEN was performed by differential pulse voltammetry (DPV) using the method described in ref. [1]. In particular, the binding of PEN resulted in conformational changes of the aptamers and as a result, MB became closer to the sensor surface that increased the current peak. Experiments were performed with different buffers, with and without NaCl, at pH 7.4 and pH 5 The optimal incubation times for the aptamer on the gold surface were also investigated. Further to that the specificity of the biosensors was studied in the presence of kanamycin, ampicillin and oxytetracycline. The limit of detection (LOD) was 0.24 ng/l.

In the case of AFM1, different surface architectures were utilized as mentioned above [3]. The LOD for these sensors was as follows: 8.47 ng/l for aptasensor 1 (determined by electrochemical impedance spectroscopy at presence of redox couple Fe^{-3}/Fe^{-4}) and 8.62 ng/l for aptasensors 2 and 3 (determined by DPV). In the case of aptasensor 1, AFM1 was also determined in real milk samples with recovery of above 78%.

Acknowledgments: This work was funded under European Union's Horizon 2020 research and innovation program through the Marie Skłodowska-Curie grant agreement No 101007299.

References

[1] Z. Yu, P. Cui, Y. Xiang, B. Li, X. Han, W. Shi, H. Yan, G. Zhang, Microchem. J. 157 (2020) 105077.
[2] B.H. Nguyen, L.D. Tran, Q.P. Do, H.L. Nguyen, N.H. Tran, P.X. Nguyen, Mat. Sci. Eng. C 33 (2013) 2229.
[3] S. Karapetis, D. Nikolelis, T. Hianik, Sensors18 (2018) 4218.
[4] T. Chalyan, L. Pasquardini, D. Gandolfi, R. Guider, A. Samusenko, M. Zanetti, G. Pucker, C. Pederzolli, L. Pavesi, IEEE J. Sel. Top. Quantum Electron. 23 (2017) 350.
[5] C.L.A. Hamula, J.W. Guthrie, H. Zhang, X.F. Li, X.C. Le, TrAC Trends Anal. Chem. 25 (2006) 681.

SC9
Detection of bacterial pathogens using multiharmonic acoustic methods and determination of their viscoelastic properties

Marek Tatarko[1*], Veronika Oravczová[1], Sandro Spagnolo[1], Judit Süle[2] and Tibor Hianik[1]

[1]Faculty of mathematics, physics and informatics, Comenius University, Mlynská dolina F1, 842 48, Bratislava, Slovakia,
[2]Hungarian Dairy Research Institute Ltd., -HDRI Ltd., Lucsony u. 24, 9200 Mosonmagyaróvár, Hungary
** Corresponding author: tatarko4@uniba.sk*

Acoustic methods are increasingly used to study the interactions of DNA aptamers with their specific targets. They represent crucial step in development of aptamer-based biosensors for monitoring of the food contamination by bacterial pathogens. We report application of the multiharmonic quartz crystal microbalance with dissipation (QCM-D) to study of the interaction of *Listeria innocua and Listeria monocytogenes* with the surface of the piezocrystal modified by DNA aptamers. QCM-D measures the changes in resonant frequency, Δf, and dissipation, ΔD, of piezocrystal at various modification of its surface. This method has been already used for detection of *Listeria innocua* and *Listeria monocytogenes* [1]. We used DNA aptamer that specifically bind to *Listeria monocytogenes*. The aptamers were modified by biotin for immobilization on a neutravidin layer chemisorbed at a gold surface of piezoelectric transducer. *Listeria* species were also applied on clean gold surface or surface containing only neutravidin layer to analyze possible not specific binding. Using Kelvin-Voigt viscoelastic model [2] we also studied viscoelastic properties of the sensing layers. At higher concentration of *Listeria innocua*, we observed anomalous increase of the resonant frequency. The frequency and dissipation changes allowed us to determine penetration depth, viscosity and elasticity values of sensing layers and to explain the anomalous frequency changes by spring like effect [3]. We also applied DNA aptamers modified by amino group for preparation of the acoustics sensors for detection *Listeria monocytogenes*. In this case the aptamers were covalently attached to the chemisorbed monolayer of 11-mercaptoundecanoic acid by means of carbodiimide chemistry. The sensor revealed significant response to *Listeria monocytogenes*, while non-specific interactions with *Listeria innocua* and *E. coli* were rather weak.

Acknowledgments: This work was funded under European Union's Horizon 2020 research and innovation program through the Marie Skłodowska-Curie grant agreement No 101007299 as well as by Science Grant Agency VEGA, project No. 1/0419/20.

References

[1] V. Oravczová, M. Tatarko, J. Süle, M. Hun, Z. Kerényi, A. Hucker, T. Hianik, Proceedings (MDPI), 60 (2020) 18.
[2] M.V. Voinova, Urban Climate, 24 (2018) 264-275.
[3] M. Tatarko, S. Spagnolo, V. Oravczová, J. Süle, M. Hun, A. Hucker, T. Hianik, Sensors (Basel), 21 (2021) 5585.

Tasks for Practical Courses

Task 1
Preparation of aptamer-based biosensors and their impedance characteristics

Lenka Bábelová[1], Veronika Oravczová[2]

[1]Institute of Animal Biochemistry and Genetics, Center of Biosciences SAS, Dúbravská cesta 9, 840 05 Bratislava, Slovakia
[2]Faculty of Mathematics, Physics and Informatics, Comenius University in Bratislava, Mlynská dolina F1, 842 48 Bratislava, Slovakia

THEORETICAL PART

Biosensors consist of a sensing layer, transducer and analyzer. The sensing layer contains receptors sensitive on materials of biological or chemical origin. The transducer converts the biological and chemical signal into electric, optic, or gravimetric signal and offers information about quantity/semiquantity of analyte. Depending on the type of transducer, we differentiate optical, electrochemical, piezoelectric and calorimetric biosensors. So far various types of receptors were used in biosensor development, such as antibodies, enzymes, nucleic acid and peptide-based aptamers, bacteriophage, ssDNA/RNA probes and more.

Aptamers were first reported in 1990 as single-stranded oligonucleotides (typicaly 30 to 100 bases), which recognize specific ligands and bind to various target molecules ranging from small ions to large proteins, viruses, bacteria or cells with high affinity and specificity. They are produced by SELEX (Systematic Evolution of Ligands by EXponential enrichment) process *in vitro* from populations of random sequences. Aptamers form characteristic 3D structures under certain conditions, such as ionic strength, pH, etc. These structures can resemble stems, loops, hairpins, triplexes or quadruplexes. This tertiary conformational structure furnishes the key for understanding of molecular interaction between the aptamer and the target. Small molecules are bound by fitting into the aptamer conformation by the formation of intermolecular hydrogen bonds. Large targets (i.e. proteins, cells) bind to the aptamer by non-covalent ligations such as hydrogen bonds, electrostatic interactions, base stacking effects and hydrophobicity.
Aptamers offer numerous advantages over antibodies:

* chemical stability under a wide range of buffer conditions
* resistant to harsh treatments without losing its bioactivity
* the thermal denaturation is reversible for aptamer
* small in size, cost effective, offering remarkable flexibility and convenience in designing their special structure

APTASENSORS

Biosensors based on aptamers as biorecognition elements - the aptasensors - are of substantial interest. In 2004, the first electrochemical aptasensor was described [1]. The crucial step in electrochemical aptasensors is the immobilization of aptamers to the electrode surface. It is important to develop strategies for reliable immobilization of aptamers so that they retain their biophysical characteristics and binding abilities, as well as for minimizing nonspecific binding/adsorption.

Aptamer immobilization techniques on the electrode surface

The control of aptamer immobilization is essential in order to ensure proper orientation, reactivity, accessibility and stability of the sensor. The achievement of high sensitivity and selectivity requires minimization of nonspecific adsorption and the stability of the immobilized aptamers. Immobilization techniques:

* physical adsorption (hydrophobic interaction)
* covalent binding (chemical binding)
* avidin-biotin affinity (specific interaction)
* self-assembled monolayers (chemical binding or adsorption)

The detection method is important for practical application of aptasensors. In this course we focus on electrochemical methods described below.

Electrochemical aptasensors

Electrochemical techniques have been extensively used as a powerful tool for fast detection of aptamer-ligand interactions due to their high sensitivity, fast response, easy operation, possibility of miniaturization, relatively compact, as well as low production cost. Aptasensors are used in numerous applications - therapeutic, drug delivery, in the field of pharmaceuticals or biological analysis (the separation techniques), bio-imaging, diagnostics.

Electrochemical impedance spectroscopy (EIS)

The term impedance was introduced by the electrical engineer, physicist and mathematician Olivier Heaviside in 1886, who adapted complex numbers to the study of electrical circuits. Impedance spectroscopy is a powerful method of analysis the complex electrical resistance of a system and is sensitive to surface phenomena and changes of bulk properties. The term impedance “spectroscopy” is derived from the fact that the impedance is generally determined at different frequencies rather than just one.

Basic principles: Theory of electrochemical impedance is a well-developed branch of ac theory that describes the response of a circuit to an alternating current or voltage as a function of frequency. In dc theory (a special case of ac theory where the frequency equals 0 Hz) resistance is defined by Ohm's law:

$$E = I\mathrm{R} \qquad (1)$$

Using Ohm's law, one can apply a dc potential (*E*) to a circuit, measure the resulting current, and calculate the resistance (*R*) - or determine any term of the equation if the other two are known. A resistor is the only element that impedes the flow of electrons in a dc circuit. In ac theory, where the frequency is non-zero, the analogous equation is:

$$E = IZ \qquad (2)$$

As in Eq. (1), *E* and *I* are defined as potential and current, respectively. *Z* is the impedance, the ac equivalent of resistance. Impedance values are also measured in Ohms (Ω). In addition to resistors, capacitors and inductors impede the flow of electrons in ac circuits. The impedance *Z* of a system is determined by applying a sinusoidal voltage with a small amplitude and detecting the current response. To

calculate the impedance of the system, an expression analogous to Ohm's law is used [2,3]:

$$Z = \frac{E(t)}{I(t)} = \frac{E_0 \sin(2\pi f t)}{I_0 \sin(2\pi f t + \varphi)} = \frac{1}{Y} \qquad (3)$$

where E_0 and I_0 are the amplitudes of voltage and current, respectively, t is the time, $\omega = 2\pi f$ is the circular frequency (f is frequency expressed in Hz), φ is the phase shift between the voltage-time and current-time functions and Y is the complex conductance or admittance.
According to Euler's expression:

$$e^{j\varphi} = \cos\varphi + j \sin\varphi \qquad (4)$$

the impedance is represented as:

$$Z = Z_0 \ (\cos\varphi + \mathrm{j} \sin\varphi) = Z_r + jZ_i \qquad (5)$$

Data presentation: The most common graphical representation of impedance data is the "Nyquist plot", in which the imaginary part of the impedance is plotted versus the real part to give a complex-plane impedance plot. In this plot, each point corresponds to a different frequency. The impedance vector with magnitude |Z| (|Z| ≡ Z_0) forms with x-axis an angle – phase angle φ (Figure 1).

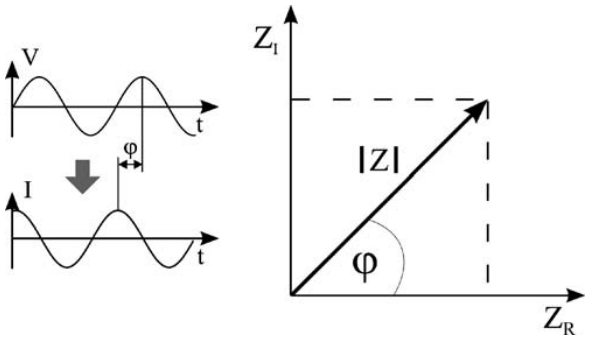

Figure 1. Impedance is a complex value that is defined as the quotient of the voltage (time) and current (time) functions. It can be expressed as the modulus |Z| and the phase angle φ, or it can be specified by the real (Z_R) and the imaginary (Z_I) parts of the impedance.

In order to characterize a biological material, e.g. antibodies or cells, electrodes must be introduced into the system, thus forming an electrochemical cell. Upon applying of an ac voltage perturbation, the current is coerced to flow through all components of the system – the working electrode, the biological material, the solution and the counter electrode. The measured impedance is the sum of all of the individual contributions. The Randles equivalent circuit fits many chemical systems. The simply Randles equivalent circuit is the starting point for other more complex models (Figure 2A).

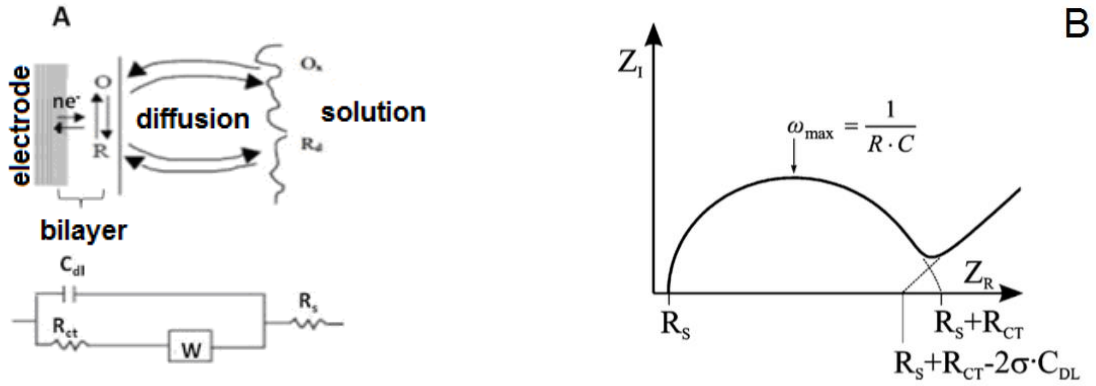

Figure 2. (A) Randles' equivalent circuit for an electrode in contact with an electrolyte. The double-layer capacitance C_{dl} results from charge being stored in the double layer at the interface. The charge transfer resistance R_{ct} refers to current flow produced by redox reactions at the interface, and the Warburg impedance, *W*, results from the impedance of the current due to diffusion from the bulk solution to the interface. R_s is the solution resistance afforded by the ion concentration and the cell geometry. R_s and R_{ct} can easily be determined from the Nyquist plot (B). The intercept is equal to $R_S + R_{ct} - 2\sigma C_{dl}$, from which σ and subsequently diffusion coefficients can be calculated.

APPARATUS

PalmSens4 Potentiostat/Galvanostat/Impedance Analyzer (PalmSens BV, Netherlands), Ultrasonicator DT 31 (BANDELIN electronic, Berlin, Germany)

Setup of the electrochemical cell:
An electrochemical workstation consists of a potentiostat and relevant control software on one end, and the electrochemical cell setup – generally inside a Faraday cage – on the other end. Electrochemical cells are designed to hold a working, reference, and counter electrode in an appropriate geometry, but beyond that they can vary a great deal.

ACCESORIES AND REAGENTS

Amino modified DNA oligonucleotide (Generi Biotech, Czech Republic), Penicillin G, 11-Mercaptoundecanoic acid (MUA), N-(3-Dimethylaminopropyl)-N'-Ethyl (EDC), N-Hydroxisuccinimide (NHS), ethanolamine phosphate buffer saline tablet (PBS), potassium ferricyanide(III) powder ($K_3Fe(CN)_6$) potassium hexacyanoferrate(II) trihydrate ($K_4Fe(CN)_6$) (Sigma Aldrich, Germany), alumina powder 1.0 µm and 0.3 µm (CH Instruments Inc., USA), ethanol (96.3%, Slavus), H_2SO_4 (96%, Slavus, Slovakia)

CHI101 2-mm-diameter gold working electrode (CH Instruments)
CHI111 Ag/AgCl/3M NaCl reference electrode (CH Instruments)
Platinum wire auxiliary electrode

PREPARATION OF SOLUTIONS AND SAMPLES

All solutions are prepared with deionized water (18 MΩ) from a Purelab Classic UV (Elga Water Systems, UK).
* Electrochemistry buffer (E-buffer): 10 mM PBS + 5 mM $K_4Fe(CN)_6$ + 5 mM $K_3Fe(CN)_6$ + 0.1 M KCl
* MUA solution: 1 mM MUA in ethanol
* EDC/NHS solution: 20 mM EDC + 50 mM NHS in water
* Aptamer (APT) solution: 1 μM in PBS
* Ethanolamine : 1M in PBS
* Polishing kit: nylon polishing pads + alumina powder + deionised water

!! Critical step: It is very important not to mix large and small particle sizes.

Pretreatment methods.

1. Mechanical polishing of gold electrodes using the polishing kit: Hold the electrode surface vertically to obtain a smooth planar surface. This is especially important with voltammetry electrodes and will ensure that the surrounding plastic is not worn unevenly. For uniform polishing is optimal eight pattern. An alternating clockwise/counterclockwise motion is also acceptable. Four step polishing procedure: alumina-water slurry of 1 μm - sonicating in ethanol for 5 min - alumina-water suspension of 0.3 μm - sonicating in ethanol for 5 min. Electrodes are sonicated to remove residual abrasive particles. The scheme of mechanical polishing of gold electrodes is shown on Figure 3.

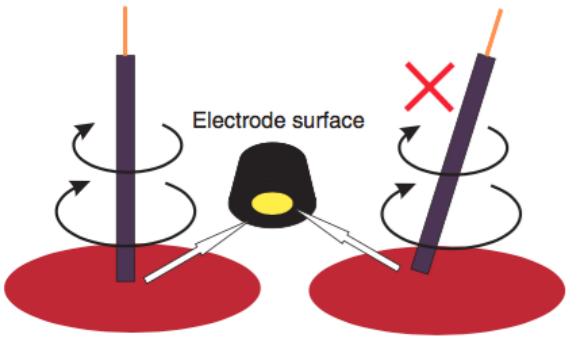

Figure 3. Schematic representations of correct electrode polishing.

However, in the case of screen-printed gold electrodes (SCPE) only the chemical cleaning is needed as described below. The SCPE integrates working, counter and reference electrode.

2. Electrochemical cleaning of gold surface. Electrochemical cleaning removes any residual impurities from the gold electrodes through electrochemical oxidation and reduction of the metal without destroying the underlying Au surfaces. This process improves electrode coverage. Place the counter, reference and working (gold) electrode in the electrochemical cell. Add 8 mL of 0.5 M H_2SO_4 into the cell.

1. *Turn on PalmSens4 and open PSTrace program on computer.*

2. *Choose method "Cyclic voltammetry"*
3. *Use scan rate of 100 mV/s.*
4. *Run 40 cycles between potential range +0.2 V to +1.5 V.*
5. *Save the cyclic voltammogram.*

A typical cyclic voltammogram for a clean, bare gold electrode is shown on Figure 4.

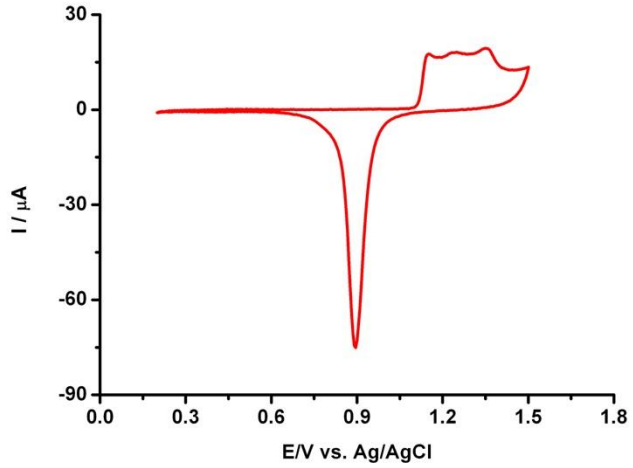

Figure 4. A typical cyclic voltammogram for a clean, bare gold electrode in a 0.5 M H_2SO_4 solution. The characteristic single sharp reduction peak located at 0.9 V and multiple overlapping oxidation peaks in the range of 1.2-1.5 V are clearly visible.

After the finishing of the electrochemical process, rinse the electrode briefly with copious amount of deionised water and dry under nitrogen stream.

!! Critical step: To avoid deposition of contaminants on the metal surface, the cleaned electrodes should be immediately used for immobilization [4].

1. **Preparation of sensing layer:**
   1. *Insert clean gold electrode in 200 µl of 1 µM MUA* in ethanol overnight (at least 12-14 h).*
   2. *Rinse the electrode with ethanol and deionised water to remove nonspecifically bound MUA.*
   3. *Incubate the electrodes for 20 minutes in a freshly prepared solution of EDC/NHS* for the activation of carboxylic acid residues.*
   4. *Rinse the electrode with PBS.*
   5. *Apply 20 µL of 1 µM aptamer* in PBS and incubate for 1h.*
   6. *Rinse the electrode with PBS.*
   7. *Apply 1M ethanolamine for 30 minutes. Ethanolamine is applied for the prevention of non-specific adsorption.*
   8. *Rinse the electrode with PBS. Electrode is ready for the application target analyte.*

   *Use freshly prepared solutions

   The scheme of the sensing layer is presented on Figure 5.

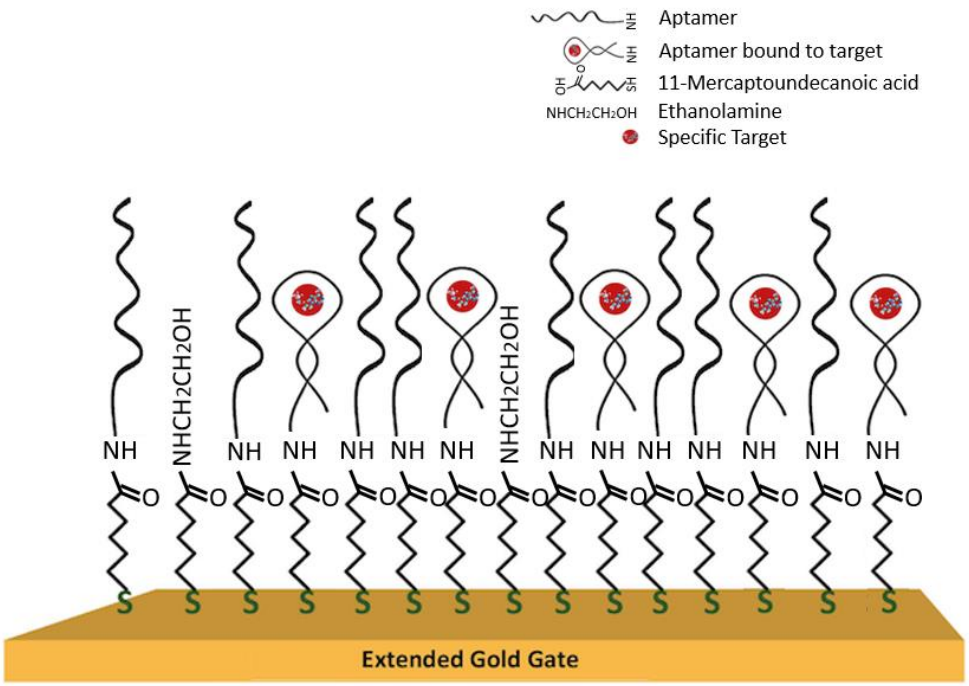

Figure 5. Schematic representation of sensing surface composed of aptamers and target molecule.

EXPERIMENT AND PARAMETERS

Electrochemical impedance spectroscopy: Place the gold electrode in the electro-chemical cell. Add 8 mL of E-buffer.

1. *Turn on PSTrace and open Impedance Spectroscopy method.*
2. *Put the following parameters:*
    a. *Frequency range: 10 kHz - 0.01 Hz.*
    b. *Amplitude signal 5 mV.*
    c. *DC potential +0.2 V*
3. *Start the experiment.*
4. *Control the data recorded.*
5. *After the measurement select "Circuit Fitting" and select the equivalent circuit diagram for the experiment.*
6. *Analyse the impedance spectrum and obtain the R_{CT} values. Evaluate.*

RESULTS

To monitor the fabrication process of biosensor and the recognition of analytes on the electrode surface, we performed EIS method, which has been widely used for monitoring the changes of electrode surface state because of its sensitive response and rapid label-free detection. Due to its nontoxicity, $[Fe(CN)_6]^{3-/4-}$ solution was used as the redox probe. To analyze the data of EIS, Nyquist diagram and the Randles equivalent circuit model were applied. The semicircle diameter of the Nyquist plot corresponds to the electron transfer resistance (R_{ct}) deriving from the resistance of the electrode surface. Therefore, R_{ct} indicates the change of the resistance properties of the layer which hinders the transfer of

redox probe to the electrode surface. The Nyquist plot of the working gold electrode of various modifications is presented on Figure 6.

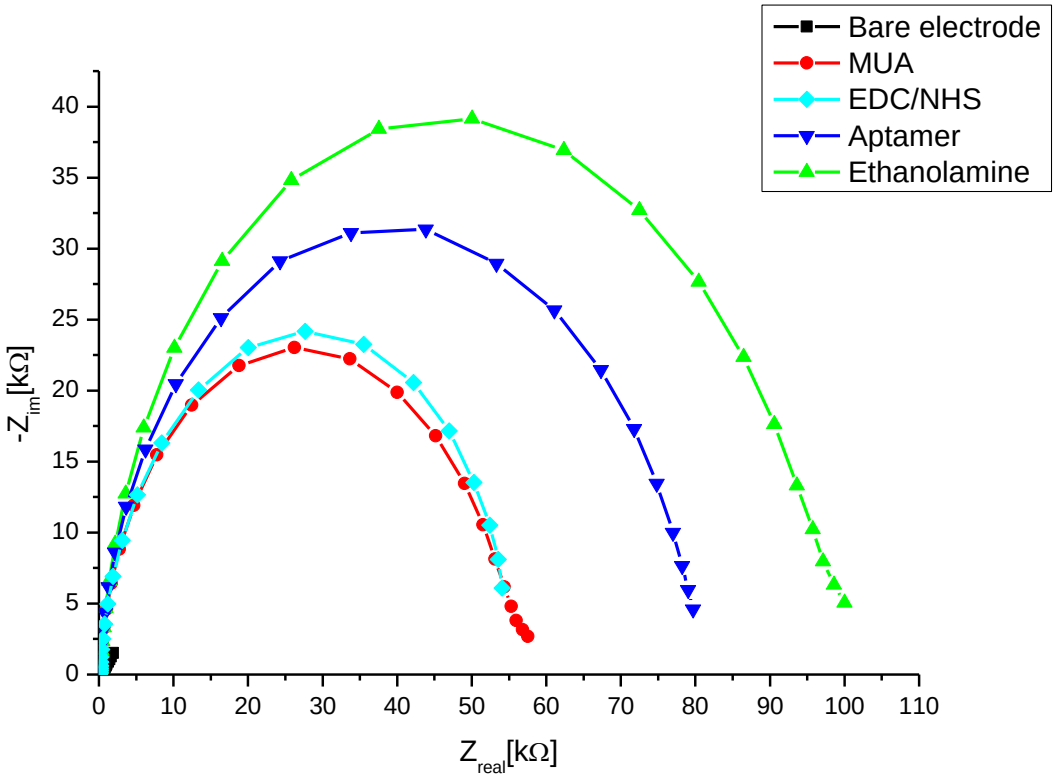

Figure 6. Typical Nyquist diagrams of EIS for fabrication and application

of the aptasensor in $[Fe(CN)_6]^{3-/4-}$ solution. EIS results were recorded for various modification steps mentioned in the *Preparation of sensing layer* starting at bare Au electrode pretreated electrochemically in 0.5 M H_2SO_4. Red line was recorded after the formation of 11-MUA SAM (self assembled monolayer), green line represents activation of carboxic acid residues using EDC/NHS, navy blue line is after immobilization of specific APT trough covalent bonds, light blue line represents blocking of unoccupied activated carboxylic acid residues.

R_{ct} for above steps fitted to the Randles equivalent circuit model (Figure 2):

Bare Au electrode: $134.8 \pm 23.4\ \Omega$.
MUA: $46.67 \pm 1.79\ k\Omega$.
EDC/NHS: $50.73 \pm 1.52\ k\Omega$.
Aptamer: $63.1 \pm 0.04\ k\Omega$.
APT+Ethanolamine: $82.0 \pm 3.28\ k\Omega$

As can be seen from Figure 6. the bare gold electrode exhibits a very small semicircle domain, suggesting a very low electron-transfer resistance to the redox marker in the electrolyte solution. The negative charge of the 11-MUA and its carboxylic acid residues positioned outwards to the solution produces an electrostatic barrier to the negatively charged redox marker $[Fe(CN)_6]^{3-/4-}$, which hinders the charge transfer processes between the redox marker in solution and the electrode. Next modification steps further increased the distance from the solution to the interface of the gold electrode, thus increasing R_{ct}. A further step of

ethanolamine backfilling completed the coverage of unoccupied activated carboxylic acid residues, thus preventing non-specific adsorption. This resulted in further increase of R_{ct} value.

REFERENCES

[1] T. Hianik, J. Wang, Electrochemical aptasensors – Recent achievements and perspectives. Electroanalysis 21 (2009) 1223-1235.

[2] D.D. Edwards, J.H. Hwang, S.J. Ford, T.O. Mason, Experimental limitations in impedance spectroscopy. Solid State Ionics 99 (2004) 85-93.

[3] F. Lisdat, D. Schäfer, The Use of electrochemical impedance spectroscopy for biosensing. Anal. Bioanal. Chem. 391 (2008) 1555-1567.

[4] S.D. Keighley, P. Li, P. Estrela, P. Migliorato, Optimization of DNA immobilization on gold electrodes for label-free detection by electrochemical impedance spectroscopy. Biosens. Bioelectron. 23 (2008) 1291-1297.

Task 2
Application of electrochemical methods for determination of the area of gold electrode and surface density of DNA aptamers

Veronika Šubjaková

Faculty of Mathematics, Physics and Informatics, Comenius University in Bratislava, Mlynská dolina F1, 842 48 Bratislava, Slovakia

THEORETICAL PART

Electrochemical methods are analytical techniques commonly used for study of the behavior of electroactive species on the electrode surface. These methods are based on measuring changes in current, potential, impedance or conductance due to redox processes at the surface.

Cyclic voltammetry (CV) is often used method for measuring an electric current as a result of oxidation–reduction process at the surface after applied a potential that is linearly increasing and decreasing in time [1]. A potential is applied to the working electrode, which changes linearly over time and has a triangle shape. Thus, the potential changes and gradually increases from a certain initial value, and then decreases to the final value. The result is a current response whose shape depends on redox processes as it is shown on Figure 1.

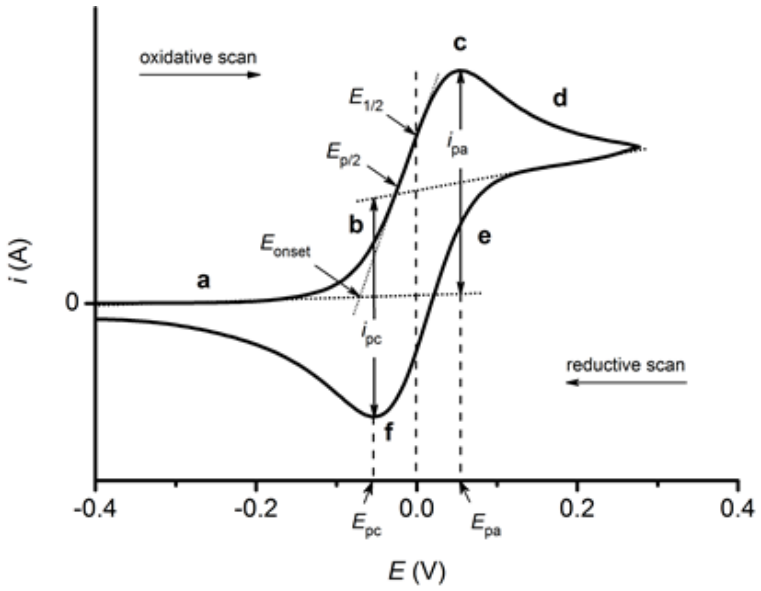

Figure 1. A cyclic voltammogram for an electrochemically reversible one-electron redox process (Source: https://www.ossila.com/en-eu/pages/cyclic-voltammetry).

From the voltammogram and the position of the current maxima (corresponding to the oxidation and reduction processes) it is possible to determine whether these are reversible, quasi-reversible or irreversible reactions. In the case of reversible reactions, these maxima are symmetric and have the same values. The amplitude of the electric current flowing through the electrode is expressed by the Randles-Sevcik equation (1)

$$I_{pa} = (2.69 \times 10^5)\, n^{2/3} A_{eff}\, D^{1/2}\, v^{1/2}\, C_0 \qquad (1)$$

where D and C_0 are the diffusion coefficient (in cm^2/s) and concentration (in mol/cm^3) of the redox probe, respectively. A_{eff} is an effective area (in cm^2), v is the potential scan rate (in V/s). The current value changes depending on the scan rate. This equation can be used for calculation of an effective area of gold electrode using solution of 1 mM $[Fe(CN)_6]^{-3/-4}$ with 0.05 M KCl. Linear plots of I_{pa} vs. $v^{1/2}$ provide evidence for a chemically reversible redox process. [2]. Other option for calculation of an effective area is based on determination of oxygen adsorption [3].

The electrochemical methods are widely used for development of biosensors. Biosensor is analytical tool that measures chemical or biological reactions by generating a measurable signal proportional to the concentration of the substance (analyte) in the reaction. The biosensor contains a receptor, a sensitive element that is biological or synthetic and specifically binds to the analyte. The example of those receptors are nucleic acid aptamers. Depending on the transducer of the signal, biosensor can be classified as electrochemical, optical or mass-sensitive.

Aptamers are single stranded DNA or RNA oligonucleotides capable to bind a target molecule with high specificity due to conformational changes in solution when fold into 3D structure forming specific binding site. Target molecules can include proteins, peptides, ions, small molecules, toxins, and even cells, viruses, and bacteria. Aptamers are widely used in biosensing as well as in the targeted drug delivery.

Quantification of DNA surface density is an important factor that affect sensitivity and performance of a biosensor. Surface density of DNA can be evaluated using redox markers such as hexaammineruthenium(III) chloride $([Ru(NH_3)_6]^{2+|3+}$ (RuHex) [2,3] or methylene blue (MB) [4,5]

The surface density of DNA aptamer labelled with MB can be calculated by determination of charge transfer, Q, responding integration of MB reduction current peak obtained from the CV scans recorded under low scan rates of 20, 50 and 100 mV/s.

$$\Gamma_{MB} = Q/nFA_{eff} \qquad (2)$$

where n is the number of electrons per molecule for reduction (n = 2 for MB) F is the Faraday constant (96 485 $C \cdot mol^{-1}$), and A_{ff} is an effective area of gold electrode. Using Γ_{MB} value it is possible to calculate surface density of DNA, Γ_{DNA} (molecules cm^{-2}):

$$\Gamma_{DNA} = \Gamma_{MB} z N_A \qquad (3)$$

where z is the charge of the redox molecules ($z = +2$ for MB) and N_A is Avogadro's number.

APPARATUS

μAUTOLAB III with FRA2 potentiostat with GPES and FRA software (Eco Chemie, The Netherlands), three electrode electrochemical cell - Teflon cell, a working gold electrode WE (diameter 2 mm, CH Instruments, USA), a reference electrode RE (Ag/AgCl), and a counter electrode CE (platinum wire), Faraday cage.

ACCESORIES AND REAGENTS

Thiol modified DNA aptamers labeled with methylene blue (MB-Apt-SH) (Generi Biotech, Czech Republic) with sequence 5′-MB-GGG TCT GAG GAG TGC GCG GTG CCA GTG AGT-SH-3´ sensitive to penicillin G [5]. $K_3[Fe(CN)_6]$, $K_4[Fe(CN)_6]$, 6-mercapto-1- hexanol (MCH), tris-(2-carboxyethyl) phosphine hydrochloride (TCEP), potassium chloride (KCl), sodium chloride (NaCl), phosphate buffer saline tablet (PBS) (137 mM NaCl, 2.7 mM KCl,10 mM phosphate buffer solution), deionised water (Purelab Classic UV, Elga Water Systems, UK), Polishing kit for gold electrode mechanical cleaning - nylon polishing pads + alumina powder with grain size 0.3 and 1 μm, ethanol, pipets, tips, gloves.

Preparation of solutions:

- 0.5 M H_2SO_4 for electrochemical cleaning of gold electrodes by CV
- Working buffer: Dissolve 1 PBS tablet in 200 mL water to obtain a 137 mM NaCl, 2.7 mM KCl and 10 mM phosphate buffer solution.
- 1 mM potassium ferro/ferri cyanide ($K[Fe(CN)_6]^{-3|-4}$) with 0.05 M KCl
- The working buffer for MB-apt-SH is 10 mM PBS containing 1M NaCl, pH = 7.4
- 1 mM 6-mercapto-1-hexanol

Immobilization of aptamers on the gold surface:
First, 10 µl of 0.5 mM TCEP was added to 10 µL of 10 µM MB-apt-SH to form a mixed solution and keep in the dark place for 1 h to reduce the disulfide bonds. Add the PBS with 1 M NaCl into mixed solution to get final concentration 1 µM of MB-apt-SH. Incubate the clean gold electrode in this solution for 1 hour, then rinse and incubate in 2 mM MCH in PBS with 1 M NaCl for overnight.

EXPERIMENT AND PARAMETERS

***Electrochemical cleaning**:*

1. *Turn on* µAUTOLAB III, computer *and open procedure CV cleaning in GPES software.*
2. *Place three electrode system in Teflon cell filled with 0.5 M H_2SO_4 solution*
3. *Measure CV in range of potential: +0.2 to +1.5 V vs. Ag / AgCl. Scan rate 0.1 V/s 20 cycles (Figure 2)*
4. *Rinse electrode with deionized water and dry by nitrogen.*

Determination of an effective area:

5. *Open procedure CV measurement*
6. *Place three electrode system in Teflon cell filled with 1 mM potassium ferro/ferri cyanide ($K[Fe(CN)_6]^{3-|4-}$) in PBS solution with 0.05 M KCl*
7. *Measure CV in range of potential: -0.2 V to +0.6 V vs. Ag / AgCl*
8. *Measure CV with scan rate: 0.1; 0.2; 0.3; 0.4; 0.5 V/s.*
9. *For each scan rate determine I_{pa}, (amplitude of the anodic peak).*
10. *Prepare dependence of I_{pa} vs. square root of the scan rate and fit with linear regression curve (Figure 3B)*
11. *Use the Randles-Sevcik equation (1) to calculate an effective area*

Electrochemical measurements for calculation of DNA surface density:

1. *Place the gold electrode with immobilized MB labeled aptamer and MCH in the electrochemical cell containing PBS with 1M NaCl.*
2. *Run CV measurement in potential range from 0 to -0.5 V with scan rate 20, 50 and 100 mV/s.*
3. *Select "Analysis" and "Integrate area" under peak from voltammogram.*
4. *Calculate the surface density of DNA using equations (2) and (3).*
5. *Discuss obtained results and compare them with the literature.*

RESULTS and EVALUATION

Electrochemical cleaning of gold electrode

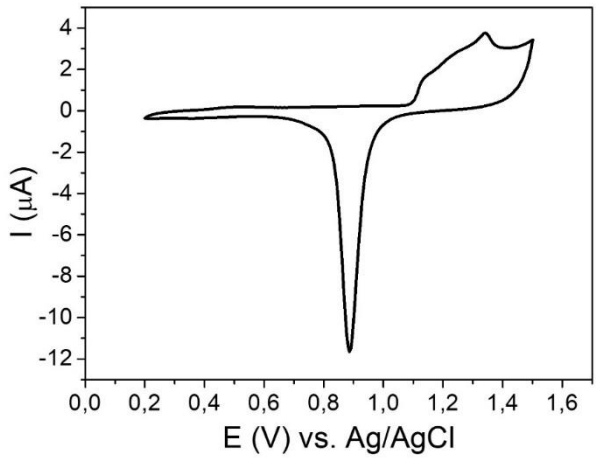

Figure 2. Typical voltammogram for electrochemical cleaning of gold electrode in 0.5 M H_2SO_4.

Determination of an effective area of gold electrode

We can determine the amplitude of anodic peaks (I_{pa}) (Figure 3A) from cyclic voltammograms obtained at different scan rates. Then we plot of I_{pa} as a function of the square root of the scan rate, which resulting in linear curve y=ax+b. (Figure 3B). Using equation (1) we can calculate an effective area of gold electrode with parameters, n = 1, D = 7.7x10^{-6} cm/s is the diffusion coefficient for 1 mM ferricyanide and C_0 = 10^{-6} M/cm^3 is the ferri/ferro cyanide concentration.

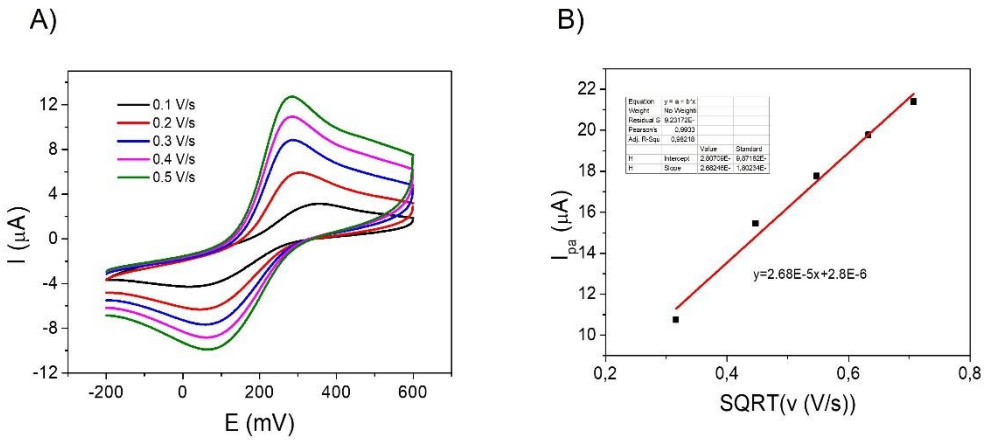

Figure 3. A) Examples of voltammogram at different scan rates, B) I_{pa} dependence on square root of scan rate.

The density of DNA aptamers at gold electrode surface

Determination of DNA density at gold surface can be calculated using equation (2) and (3) using cyclic voltammetry and the properties of the redox probe methylene blue, which is conjugated with DNA aptamer. In the work [5] for 1 μM MB-apt-SH aptamer coverage this has been calculated $(1.2 \pm 0.1) \times 10^{12}$ molecules/cm^2.

REFERENCES

[1] V. Subjakova, V. Oravczova, M. Tatarko, T. Hianik, Advances in electrochemical aptasensors and immunosensors for detection of bacterial pathogens in food, Electrochim. Acta. 389 (2021) 138724.

[2] G. Castillo, I. Lamberti, L. Mosiello, T. Hianik. Impedimetric DNA aptasensor for sensitive detection of Ochratoxin A in food. Electroanalysis 24 (2012), 512 – 520.

[3] M.-N. Nan, Y. Bi, H.-L. Xue, H.-T. Long, S.-L. Xue, L.-M. Pu, D. Prusky, Modification performance and electrochemical characteristics of different groups of modified aptamers applied for label-free electrochemical impedimetric sensors, Food Chem. 337 (2021) 127761.

[4] Y. Liu, N. Tuleouva, E. Ramanculov, A. Revzin, Aptamer-based electrochemical biosensor for interferon gamma detection, Anal. Chem. 82 (2010) 8131–8136.

[5] Z. Yu, P. Cui, Y. Xiang, B. Li, X. Han, W. Shi, H. Yan, G. Zhang, Developing a fast electrochemical aptasensor method for the quantitative detection of penicillin G residue in milk with high sensitivity and good anti-fouling ability. Microchem. J. 157 (2020) 105077.

Task 3
Aptasensors based on multiharmonic quartz crystal microbalance with dissipation (QCM-D)

Marek Tatarko

Faculty of Mathematics, Physics and Informatics, Comenius University in Bratislava, Mlynská dolina F1, 842 48 Bratislava, Slovakia

THEORETICAL PART

Conventional quartz-crystal microbalance (QCM) is basic acoustic gravimetric technique that has a broad spectrum of applications in various fields, especially in development of affinity biosensors. It utilizes AT-cut quartz crystal with gold electrodes that cover its central part on both sides. When high-frequency voltage is applied via contact of gold electrodes, it causes transverse shear oscillation in the crystal with fundamental resonant frequency f_0. Oscillation with higher harmonic frequencies f_n can be produced as well, where n is harmonic number. Such acoustic method is called multiharmonic QCM. The scheme of measuring system based on SARK110 vector analyzer is presented on Figure 1 and the scheme of the shear wave propagation is on Figure 2 [1].

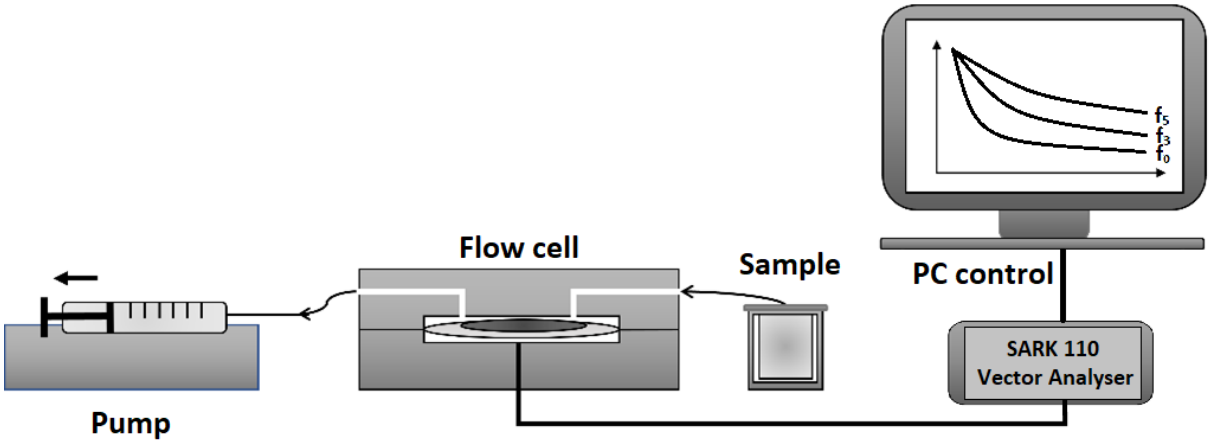

Figure 1. The scheme of multiharmonic QCM settings. Pump is pulling sample through flow cell containing QCM crystal that is connected to SARK 110 vector analyzer. Measurement is controlled by PC.

The measured frequencies depend on the interaction of molecules with the gold surface of the crystal, or with other already adsorbed species, for example antibodies or DNA aptamers. Adsorption of molecules on the crystal causes decrease in the resonant frequency. The desorption causes the frequency increase. Frequency changes under optimal conditions (blocking the naked surface and exclusion of non-specific interactions) allowing to study the interactions between immobilized molecules and applied sample. These interactions can vary from cleaving of the immobilized molecules, for example proteins at presence of proteases, or to the formation of complexes, for example between immobilized DNA aptamers and their target. By recording the changes in fundamental frequency, it is possible to estimate adsorbed mass on the crystal surface using Sauerbrey equation (1) [2]:

$$\Delta f = -\frac{2nf_0^2}{\sqrt{\rho_q \mu_q}} \frac{\Delta m}{A} = -2.26\text{x}10^{-6}\, f_0^2\, \Delta m/A \qquad (1)$$

where f_0 is fundamental resonant frequency (Hz), *A* is active crystal area (typically 0.2 cm^2), *Δf is* frequency change (Hz), ρ_q *is* quartz density (2.648 $g.cm^{-3}$), *Δm is* mass change (g) and μ_q *is* shear modulus of quartz ($2.947\text{x}10^{11}$ $g.cm^{-1}.s^{-2}$).

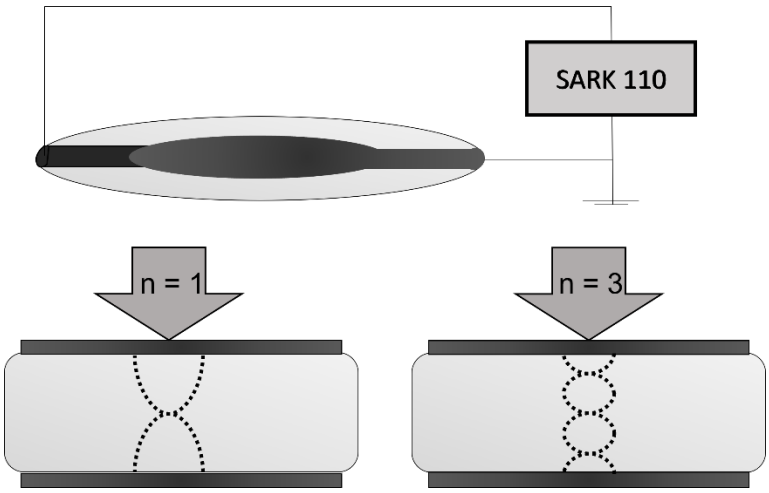

Figure 2. The scheme of the quartz crystal connected to SARK 110 vector analyzer (upper part) and the oscillation profiles for fundamental and 3rd harmonic frequencies in a quartz crystal, respectively (lower part).

Surface density of the molecules, for example neutravidin (NA) can be calculated as:

$$N = (N_A\, \Delta m) / (A.M_W) \qquad (2)$$

where *N* is surface density of NA molecules (cm^{-2}), M_W is molecular weight of NA (66 kDA), N_A is Avogadro's number ($6.022\text{x}10^{23}$ mol^{-1}) and *A* is active crystal area.

Gold electrodes allows immobilization by chemisorption of the thiol-based molecules, such as mercapto-compounds, that forms self-assembling monolayers (SAM) and serve as linkers for immobilization of another molecules. Neutravidin is deglycosylated avidin that contains thiol groups and can be therefore easily immobilized at the gold surface. NA has high affinity to biotin. Therefore, the SAM composed of NA can be used for immobilization of biotin-modified molecules [3]. This approach is used for example for preparation of biosensors based on biotinylated DNA aptamers or antibodies.

Kinetics of dissipation changes is also recorded, providing information about viscoelastic properties of the layer [4]. Frequency and dissipation can be modelled by Kelvin-Voigt viscoelastic model using equations (3) and (4):

$$f \approx -\frac{1}{(2\pi\rho_0 h_0)}\left[\left(\frac{\eta_3}{\Gamma_3}\right) + h_1\rho_1\omega - 2h_1\left(\frac{\eta_3}{\Gamma_3}\right)^2\left(\frac{\eta_1\omega^2}{\mu_1^2} + \omega^2\eta_1^2\right)\right] \qquad (3)$$

$$\Delta D \approx \frac{1}{(\pi f_n \rho_0 h_0)}\left[\left(\frac{\eta_3}{\Gamma_3}\right) + 2h_1\left(\frac{\eta_3}{\Gamma_3}\right)^2\left(\frac{\eta_1\omega}{\mu_1^2} + \omega^2\eta_1^2\right)\right] \quad (4)$$

where Γ_3 is the decay length of the shear wave in the liquid; ρ_3 and η_3 are the density and viscosity of the liquid (water or very dilute saline solutions have similar density, 0.9982 g/cm^3, and dynamic viscosity, 1.0016 mPa·s, at 20 °C), ρ_0 = 2.648 g·cm^{-3} and h_0 = 0.208 mm (for the crystal with fundamental frequency f_0 = 8 MHz) are the density and thickness of the quartz crystal, respectively. h_1, μ_1, η_1 and ρ_1 are the thickness, the shear modulus, viscosity, and density of the adsorbed film, respectively; $\omega = 2\pi f$ is the angular frequency of the oscillation.

In this task the formation of neutravidin layer will be monitored on the clean gold surface of the QCM crystal and the surface density of NA molecules will be determined together with the viscoelastic values of the NA layer.

APPARATUS

Multiharmonic QCM method utilizes a vector analyzer SARK-110 (Seeed, Shenzhen, China) to determine resonant frequency f and dissipation D. AT-cut crystal (Total Frequency Control, Ltd., UK) with fundamental resonance frequency of 8 MHz with working electrode area 0.2 cm^2 is placed to flow cell with inner volume of 100 µL and 50 µl/min flow is applied by digital pump Genius Touch (Kent Scientific, USA). The scheme of apparatus with a flow cell is on Figure 1.

ACCESSORIES AND REAGENTS

Deionized water, Neutravidin (THP Medical Products, Austria), scintillation vials, syringe.

PREPARATION OF SOLUTIONS AND SAMPLES

Before measurement, AT-cut crystals were cleaned in basic Piranha solution (5:1:1 deionized water, hydrogen peroxide and ammonia), rinsed in deionized water and ethanol and eventually dried by nitrogen stream before inserting into the cell. Neutravidin is diluted to 0.125 mg/ml in deionized water. Volume of this sample must be at least 2 ml.

EXPERIMENT AND PARAMETERS

1. Measurement is initiated by wash of the crystal surface in a flow cell with deionized water.
2. When resonant frequency and dissipation become stable, deionized water is exchanged for 0.125 mg/ml aqueous solution of neutravidin (Figure 3a).
3. Neutravidin dissolved in deionized water is applied for 35 minutes to react sufficiently with gold surface (Figure 3b)
4. Neutravidin is replaced by deionized water.
5. Deionized water is left to flow through the cell for at least 20 minutes to achieve stabile characteristics after unbound neutravidin is being washed off from the crystal surface (Figure 3c).

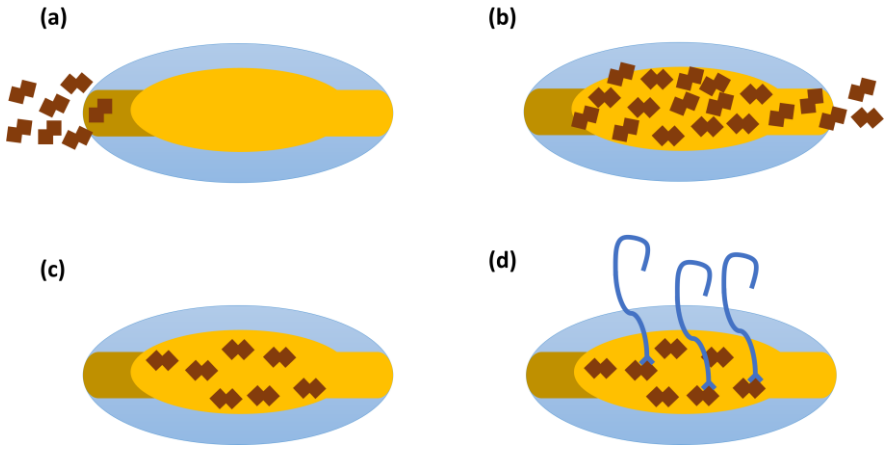

Figure 3. The scheme of immobilization of neutravidin. Neutravidin is applied on clean crystal (a) until sufficient coverage of gold surface is achieved (b). Crystal is washed with deionized water to remove unbound neutravidin (c). (d) example of the sensing surface with biotinylated aptamers bonded to the neutravidin monolayer.

EVALUATION

Fundamental resonant frequency before and after addition of neutravidin are recorded (Figure 4a) and using Sauerbrey equation (1) the mass density is estimated. Change of both frequency and dissipation for several harmonics are used in Kelvin-Voigt model to calculate changes in viscoelastic properties – penetration depth, viscosity coefficient and shear modulus.

RESULTS AND DISCUSSION

Kinetics of resonant frequency and dissipation following chemisorption of neutravidin (NA) are measured and used for determination of NA surface density, penetration depth, viscosity coefficient and shearing modulus. Example of the kinetics changes of the resonant frequency, 3rd and 5th harmonics frequencies following addition of NA and washing of the surface by deionized water is shown on Figure 4a. Addition of NA resulted in sharp decrease of resonant frequency and higher harmonics frequencies. After approx. 35 min. the steady-state values of frequencies (Figure 4a) and dissipation (Figure 5) were observed. Subsequent washing of the surface by deionized water resulted in removal of weakly adsorbed NA molecules, which cause small increase of frequency and decrease of dissipation (Figure 5). The Sauerbrey equation is used for quantification of the mass gain or loss of rigid and thin adlayers from the changes in the resonant frequency of the QCM. The stiffness of the adlayer influences the elastic and energy lossless propagation of the acoustic wave, whereas its thickness affects the time in which the wave propagates at a different speed in the adlayers. The thinner the layer is, the shorter is the time during which the wave propagates at a different speed, thus allowing this difference to be neglected for the calculation. Consequently, to confirm the acceptability of the equation (1), we constructed a plot of $\Delta f_n/n$ for different harmonics vs. time (Figure 4b). It can be expected that for relatively rigid layers the ratio $\Delta f_n/n$ at different overtones should not differ [5], which we certainly observed.

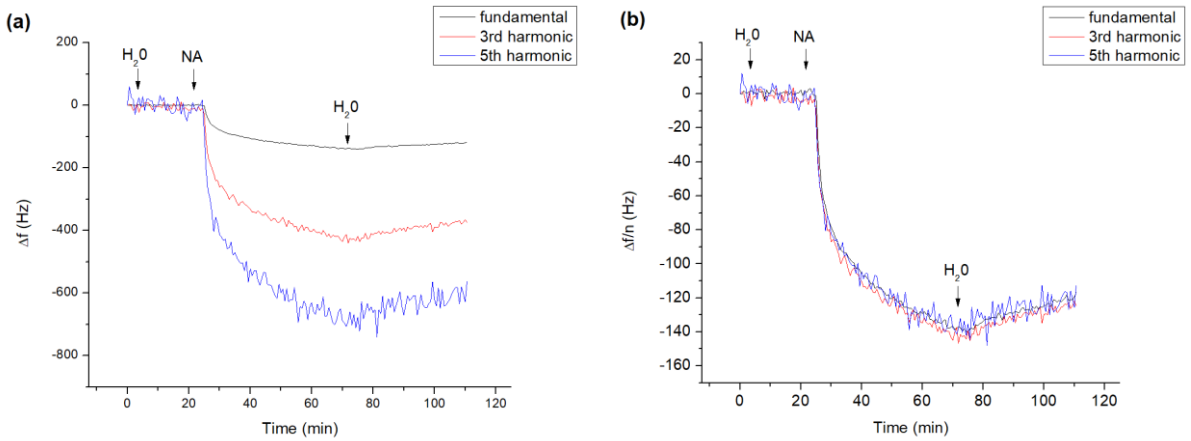

Figure 4. The kinetics of changes of (a) fundamental frequency and the 3rd and 5th harmonics. (b) normalized frequency changes following addition of 0.125 mg/ml neutravidin (NA) on gold surface of quartz crystal and washing with deionized water (H_2O).

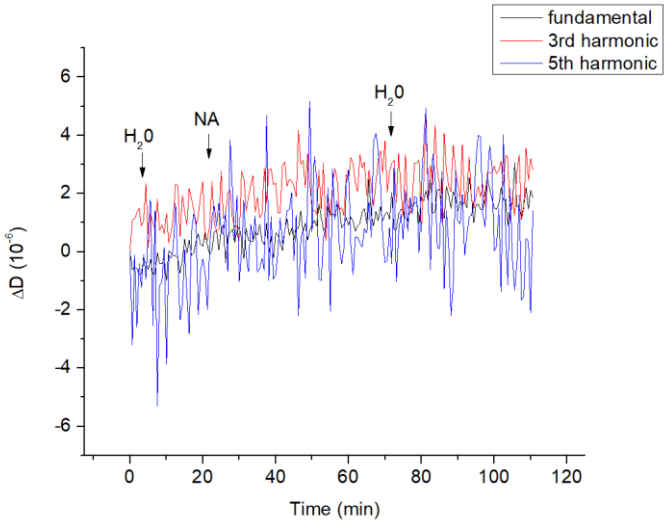

Figure 5. The kinetics of changes of dissipation, ΔD, at fundamental frequency, 3rd and 5th harmonics following addition of 0.125 mg/ml neutravidin (NA) on gold surface of quartz crystal and wash with deionized water (H_2O).

Thus, the total changes of resonant frequency, corresponding to the formation of stable NA layer is Δf = -121 Hz, confirming NA mass deposition on a gold surface. Mass density of NA calculated using Sauerbrey equation (1) is 0.84 μg.cm^{-2}. Consequently, using equation (2), surface density is 7.66 x 10^{12} NA molecules.cm^{-2}.

Obtained values of 3rd and 5th harmonics and dissipation can be used for evaluation of viscoelastic values of the NA layer using Excel spreadsheet for Kelvin-Voigt model calculations. After setting of the boundary condition, values of penetration depth, viscosity and shear modulus are determined for crystal without and with NA layer. Following adsorption of NA, the penetration depth decreased from about 250 nm to 120 nm. This is evidence that neutravidin forms a very compact layer. This is also accompanied by increase of the viscosity coefficient by about 1.42 mPa·s. This viscosity increase is evidence of certain friction of NA layer with surrounding water. The adsorption of NA resulted in the increase of the shear modulus by 3.6 × 10^5 Pa, which is due to the formation of a compact structure [6,7].

REFERENCES

[1] T.E. Alexander, L.D. Lozeau, T.A. Camesano, QCM-D characterization of time-dependence of bacterial adhesion. The Cell Surface 5 (2019) 100024.

[2] J. Kankare, Sauerbrey equation of quartz crystal microbalance in liquid medium. Langmuir 18 (2002) 7092-7094.

[3] A.T. Marttila, O.H. Laitinen, K.J. Airenne, T. Kulik, E.A. Bayer, M., Wilchek, M.S. Kulomaa, Recombinant NeutraLite avidin: a non-glycosylated, acidic mutant of chicken avidin that exhibits high affinity for biotin and low non-specific binding properties. FEBS Lett 1 (2000) 31-36.

[4] M.V. Voinova, Modelling of the response of acoustic piezoelectric resonators in biosensor applications – Part 1: The general theoretical analysis. J. Sens. Sens. Syst. 4 (2015) 137–142.

[5] S. Spagnolo, E.S. Muckley, I.N. Ivanov, T. Hianik, Analysis of trypsin activity at β-casein layers formed on hydrophobic surfaces using a multiharmonic acoustic method. Analyst 147 (2022) 461.

[6] M. Tatarko, S. Spagnolo, V. Oravczová, J. Süle, M. Hun, A. Hucker, T. Hianik, Changes of viscoelastic properties of aptamer-based sensing layers following interaction with *Listeria innocua*. Sensors (Basel) 21 (2021) 5585.

[7] J.S. Ellis, M. Thompson, Viscoelastic modeling with interfacial slip of a protein monolayer electrode-adsorbed on an acoustic wave biosensor. Langmuir 26 (2010) 11558 – 11567.

Task 4
Application of colorimetry for detection of analytes

Ivan Piovarči

Faculty of Mathematics, Physics and Informatics, Comenius University in Bratislava, Mlynská dolina F1, 842 48 Bratislava, Slovakia

THEORETICAL PART

Colorimetric biosensor detects analyte based on changes in the wavelength and subsequent changes in the color of the sample. Usually, the wavelength of the light used in colorimetry is in the range of 400-700 nm, which is visible to the naked eye. These types of biosensors are usually rapid and easy to use. This is advantageous for *point-of-care* analysis [1]. One of the more common and famous colorimetric biosensors are based on the lateral flow principle (Figure 1). The examples of such sensors are antigen tests against SARS-CoV-2 or pregnancy test. They are based on the interaction of antibodies modified with metal or latex nanoparticles or fluorescent tags with the sample [2]. The sample is dropped on the cellulose membrane and transported by means of capillary forces through the testing and control strip. If the analyte of interest is present, the testing strip will capture it and present itself as a colored strip. The control strip is specific for the color producing molecules.

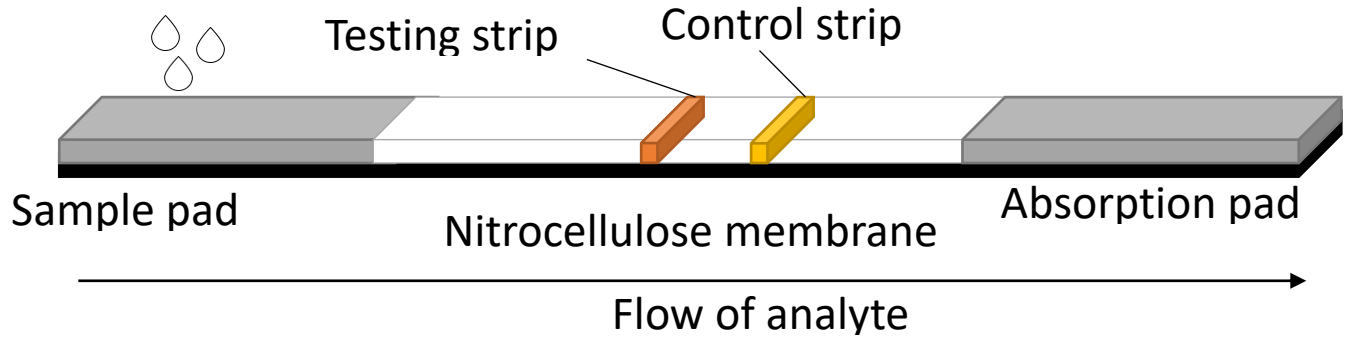

Figure 1 Scheme of lateral flow colorimetric biosensor.

The sources of color signal in colorimetric biosensors can be different, ranging from metal nanoparticles to various chromogenic enzyme substrates. In this practical task we will use gold nanoparticles (AuNPs). These nanoparticles have ability to absorb visible light due to surface plasmon resonance effect (SPR) or localized surface plasmon resonance (LSPR) [3]. This effect arises from the oscillating electromagnetic field of light that contacting with the free electrons in metallic nanoparticles and induces their coherent oscillations. This causes strong optical absorption in UV-vis part of the spectrum. The SPR absorbance of AuNPs depends on the surrounding medium and on the distance between nanoparticles. It is usually characterized by a maximum of absorbance around 520 nm (Figure 2). Well dispersed AuNPs will absorb mainly in the blue part of the visible spectrum and thus will present a red color in colloid solution. During aggregation the AuNPs get closer together, start to absorb more in red part of the visible spectrum and thus present blue color. This color change during AuNPs aggregation is easily visible by naked eye and thus serves as a good signal for evaluation of molecular interactions in a

colorimetric assay. Using Mie theory one can calculate the size and concentration of nanoparticles by means of equations (1) and (2) [4].

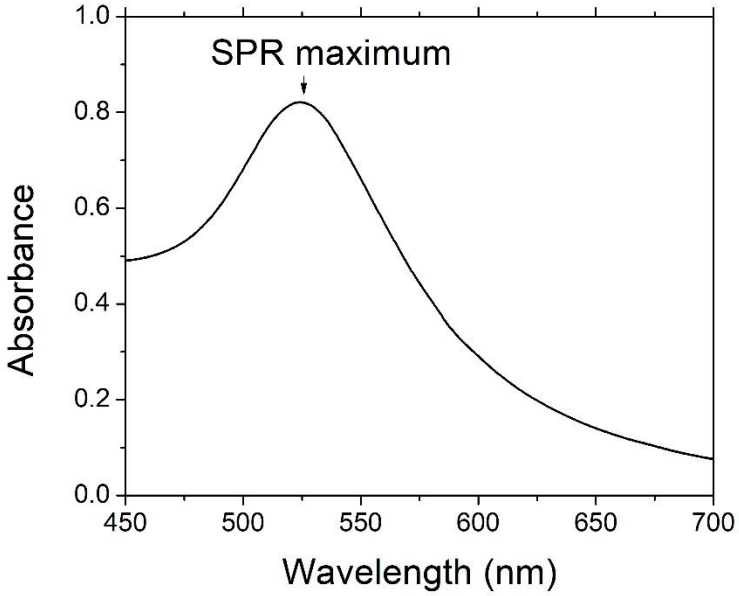

Figure 2. The example of AuNPs spectrum.

As an input parameter the ratio of absorbance at wavelength 450 nm and absorbance at the peak position is used.

$$d = e^{\left(B_1 \frac{A_{spr}}{A_{450}} - B_2\right)} \tag{1}$$

$$N = \frac{A_{450} \times 10^{14}}{d^2 \left(-0.295 + 1.36 e^{-\left(\frac{d-96.8}{78.2}\right)^2}\right)} \tag{2}$$

Where *d* is diameter of the nanoparticles in nm B1 and B2 are constants (B_1 = 3.00 and B_2 = 2.20), A_{spr} is absorbance at SPR maximum, A_{450} is absorbance at 450 nm wavelength. N is number of nanoparticles per 1 ml. There exist various methods of AuNPs synthesis. One of the first belongs to Turkevich et al. [5], which in 1951 presented a detailed method of the preparation of AuNPs. This method is now a cornerstone for AuNPs preparation. In this method, a reduction of Au ions into Au atoms was used. AuNPs in solution have different stability and tend to aggregate depending on the suspension and surface modification. AuNPs can be stabilized electromagnetically or sterically. Electromagnetic stabilization is produced by charge of the surface ligands of AuNPs, either positive or negative. It is assumed that the Z-potential should be at least +20 or −20 mV, respectively, for the AuNPs to be stable. Another way to stabilize AuNPs is steric stabilization, which is commonly achieved by using surfactants, for example Tween-20, Tween-80, sodium dodecyl sulfate (SDS) and others. In the synthesis of the AuNPs by reduction method, it is necessary to use chemicals for the reduction of Au^{3+} and Au^{1+} ions to Au^0, as well as a corresponding stabilizing agent. The Turkevich method is an easy, efficient and relatively precise method for synthesis of AuNPs and therefore it is most widely used [5]. In short, this method consists of heating the solution of gold chloride ($HAuCl_4$) to a boil and adding sodium citrate. It is based on a seed-mediated process. The

sodium citrate acts both as a reduction agent and stabilizer for the gold nanoparticles.

APPARATUS

- UV-vis spectrophotometer
- Magnetic stirrer and hotplate

ACCESORIES AND REAGENTS

$HAuCl_4$ 250 mM in distilled water, sodium citrate trihydrate 39 mM in distilled water, β-casein 1 mg/ml in distilled water, 5 M NaCl in distilled water (Deionized water is recommended). Chemical used are from Sigma-Aldrich (Germany).

EXPERIMENT AND PARAMETERS

- Prepare 20 ml of 0.25 mM $HAuCl_4$ solution by mixing 20 μl of 250 mM $HAuCl_4$ in 19.98 ml of distilled water.
- Heat the solution at around 90-95 ^oC for 20 minutes.
- Quickly add 680 μl of 39 mM of trisodium citrate.
- Leave the solution at the hotplate for around 25-30 minutes. Remove it from the hotplate and cooldown after at room temperature.
- Measure the absorbance spectrum from 450 nm to 700 nm. Calculate the size and concentration using equation (1) and (2), respectively.
- Add 100 μl of 1 mg/ml of β-casein to one sample and measure the change of the spectrum
- Add 50 μl of 5 M NaCl to both samples
- See and measure the change of color and spectrum of the sample

EVALUATION

During the experiment, we synthetize AuNPs using Turkevich method which produces gold nanoparticles of sizes from 5-50 nm depending on the conditions of the experiment. We then characterize those AuNPs using UV-vis spectrophotometer by finding the absorbance at SPR peak (around 520 nm) and absorbance at 450 nm. Using equations (1) and (2) it is then possible to calculate the approximate size and concentration of the nanoparticles. In our example we calculated the size to be approximately 17 nm at concentration of 1.5 nM. We then added 100 μl of milk protein, β-casein, to 1 ml of the sample and measured the spectrum again. The shift of the maximum from 524 nm to 526 nm is observed (Figure 3). This shift arises from the interaction of β-casein with the surface of AuNPs. Then we added 50 μl of 5 M NaCl to a sample of AuNPs with β-casein and to AuNPs sample without this protein. The NaCl induces the color change of the sample not containing β-casein. This due to the fact, that without protein the AuNPs aggregates following addition of NaCl. This is since high concentration of salts decreases the screening length of charged chemical groups on the surface of AuNPs and thus induce their aggregation. The examples of spectra and color change are presented in Figure 3.

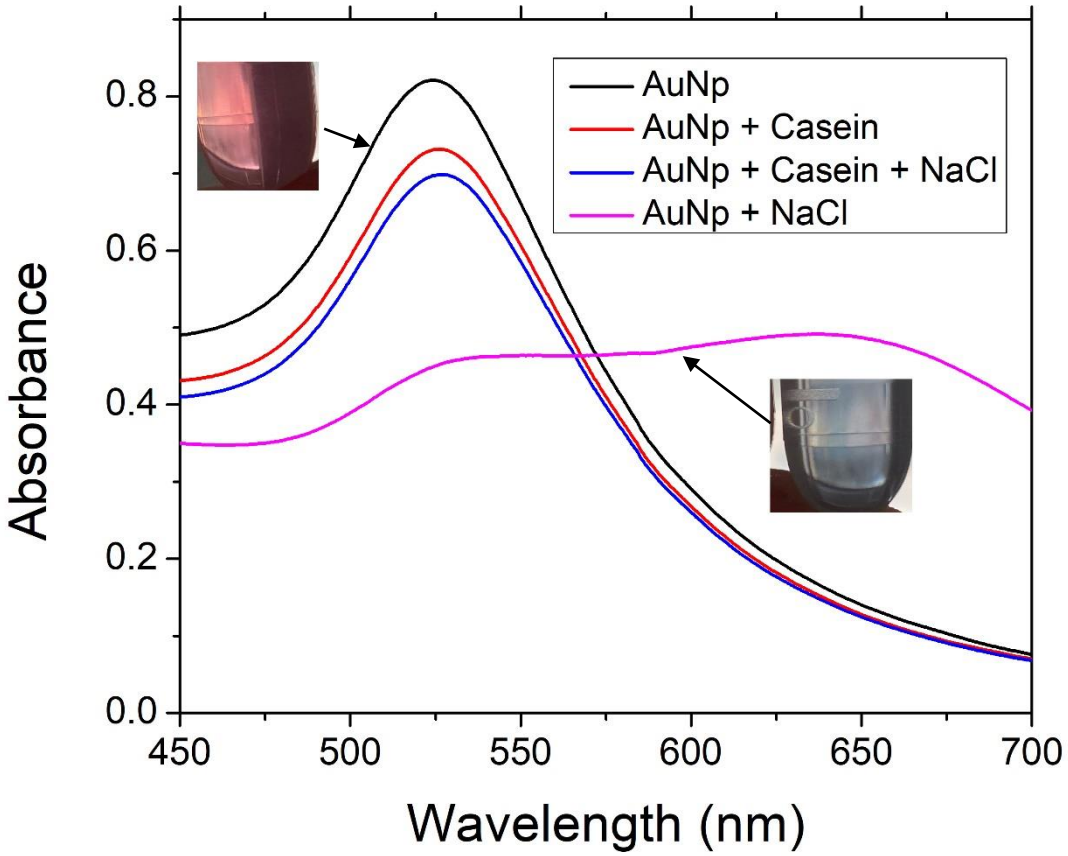

Figure 3 Example of absorbance spectra for AuNPs with associated color changes.

The concept of AuNPs aggregation and their protection from it due to an interaction with an analyte is the basis for different colorimetric methods in solution. For example, it is possible to modify the AuNPs with β-casein further with mercaptohexanol, which destabilizes the surface charge of the AuNPs. After addition of a protease specific for casein, for example trypsin or plasmin, the MCH molecules are no longer fully covered with β-casein which leads to their aggregation [6]. Molecules such as DNA or RNA can also non-specifically interact with the surface of gold nanoparticles, protecting them from salt-induced aggregation. This can be used in colorimetric aptasensors for detection bacterial pathogens. In this assay the specific aptamers are first incubated with the bacteria. After the incubation, the sample is centrifuged, and supernatant is incubated with the AuNPs. Depending on the concentration of bacteria, different concentration of aptamers is present in the supernatant, with the rest being bound on bacteria in pellet. This resulted in a different colorimetric response of the AuNPs to addition of salt, depending on the concentration of the aptamer left in the supernatant and thus inversely proportional to the concentration of bacteria [7].

RESULTS

The aim of this task is to demonstrate how to prepare AuNPs, analyze their size and concentration with spectrophotometric method and observe the color change of the AuNPs suspension due to interactions with various molecules.

REFERENCES

[1] V. X. T. Zhao, T. I. Wong, X. T. Zheng, Y. N. Tan, and X. Zhou, Colorimetric biosensors for point-of-care virus detections, *Materials Science for Energy Technologies*, vol. 3, pp. 237–249, 2020, doi: 10.1016/j.mset.2019.10.002.

[2] K. M. Koczula and A. Gallotta, Lateral flow assays, *Essays in Biochemistry*, vol. 60, no. 1, pp. 111–120, Jun. 2016, doi: 10.1042/EBC20150012.

[3] H. Aldewachi, T. Chalati, M. N. Woodroofe, N. Bricklebank, B. Sharrack, and P. Gardiner, Gold nanoparticle-based colorimetric biosensors, *Nanoscale*, vol. 10, no. 1, pp. 18–33, 2018, doi: 10.1039/C7NR06367A.

[4] W. Haiss, N. T. K. Thanh, J. Aveyard, and D. G. Fernig, Determination of size and concentration of gold nanoparticles from UV−Vis spectra, *Anal. Chem.*, vol. 79, no. 11, pp. 4215–4221, Jun. 2007, doi: 10.1021/ac0702084.

[5] J. Kimling, M. Maier, B. Okenve, V. Kotaidis, H. Ballot, and A. Plech, Turkevich method for gold nanoparticle synthesis revisited, *J. Phys. Chem. B*, vol. 110, no. 32, pp. 15700–15707, Aug. 2006, doi: 10.1021/jp061667w.

[6] I. Piovarci, S. Melikishvili, M. Tatarko, T. Hianik, and M. Thompson, Detection of sub-nanomolar concentration of trypsin by thickness-shear mode acoustic biosensor and spectrophotometry, *Biosensors*, vol. 11, no. 4, p. 117, Apr. 2021, doi: 10.3390/bios11040117.

[7] I. Piovarci, J. Süle, M. Angelopoulou, P. Petrou, L. Bousiakou, S. E. Kakabakos, T. Hianik, Application of optical and acoustic methods for the detection of bacterial pathogens using DNA aptamers as receptors, in *The 2nd International Electronic Conference on Biosensors*, Feb. 2022, p. 6. doi: 10.3390/IECB2022-12268.

Task 5
Dynamic light scattering for biophysical characterization of salt-induced aggregation of gold nanoparticles. The effect of β-casein

Zuzana Garaiová

Faculty of Mathematics, Physics and Informatics, Comenius University in Bratislava, Mlynská dolina F1, 842 48 Bratislava, Slovakia

THEORETICAL PART

Gold nanoparticles (AuNPs) gain an increased interest in the nanotechnology [1]. They have unique chemical and optical properties, such as surface plasmon resonance effect (SPR). Due to SPR, AuNPs are characterized by enhanced light absorption and scattering properties. In particularly, a tunable color change from red to blue upon the increased nanoparticle size or due to the aggregation take place (Figure 1). Such a color change of AuNPs has been widely used in colorimetric biosensors [2]. Moreover, the enhanced light absporption and scattering can be also applied for imaging and cancer therapy. For example, Sun et al. [3] reported a new class of near infra red photothermal transducers with high efficiency for cancer imaging and photothermal therapy (PTT) based on salt induced AuNPs aggregation. To note, high concentration of salts in aqueous solutions can decrease the screening length of charged chemical groups on the surface of AuNPs and induce their aggregation behaviour. In the above mentionted PTT study a salt induced aggregation was desirable. Hovewer, in some other cases, various stabilizers or additional surface modifiers can be used to avoid uncontrolled growth or aggregation during the nanoparticle preparation or for post-processing application adjustment. The conjugation of nanoparticles by proteins might provide a long-term stability of the system as well as introduce biocompatible functionalities for further biological application. Caseins – comprising about 80 % of milk total protein, are a family of proteins that can naturally self-organize in the aqueous solutions, form structures called micelles and potentially stabilize the AuNPs (Figure 1) [4].

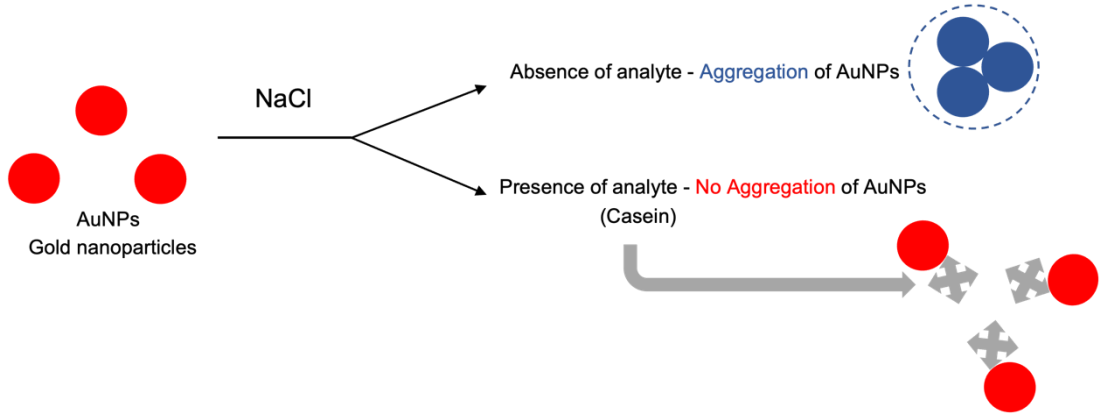

Figure 1. Schematic illustration of AuNPs upon the NaCl salt-induced aggregation in the absence and presence of stabilizing analyte – casein.

Size of AuNPs and their salt-induced/analyte-protective aggregation behaviour can be analyzed by dynamic light scattering (DLS) method [5]. DLS also known as photon correlation spectroscopy (PCS), measures Brownian motion and relates this to the size of particles. It does this by illuminating the particles with a beam of monochromatic light passed through the sample. The Brownian motion of particles in suspension causes laser light to be scattered at different intensities. The time dependent fluctuations in intensity of scattered light are then analyzed and yields the velocity of the Brownian motion called translational diffusion coefficient *D*. This coefficient is then converted into the hydrodynamic diameter D_H using the *Stokes-Einstein relationship*,

$$D_H = \frac{kT}{3\pi\eta D} \qquad (1)$$

where *k* is the Boltzmann constant, *η* is viscosity of the solvent and *T* is the temperature of the medium.

Figure 2 shows a typical DLS system comprising laser as a light source to illuminate the sample particles within the cell. Detectors measure the intensity of the scattered light and can be arranged in the position of 173° or 90°. To overcome detector to be overloaded, attenuator is used to reduce intensity of the laser, hence measuring the intensity of scattered light within a specific range for detector. From the detector, the scattering intensity signal then passes to a digital signal processing board called correlator. The correlator compares the scattering intensity at successive time intervals to derive the rate at which the intensity is varying. The correlator information then passes to the computers, where special algorithms are used to extract the decay rates for a variety of size classes to produce a size distribution [6].

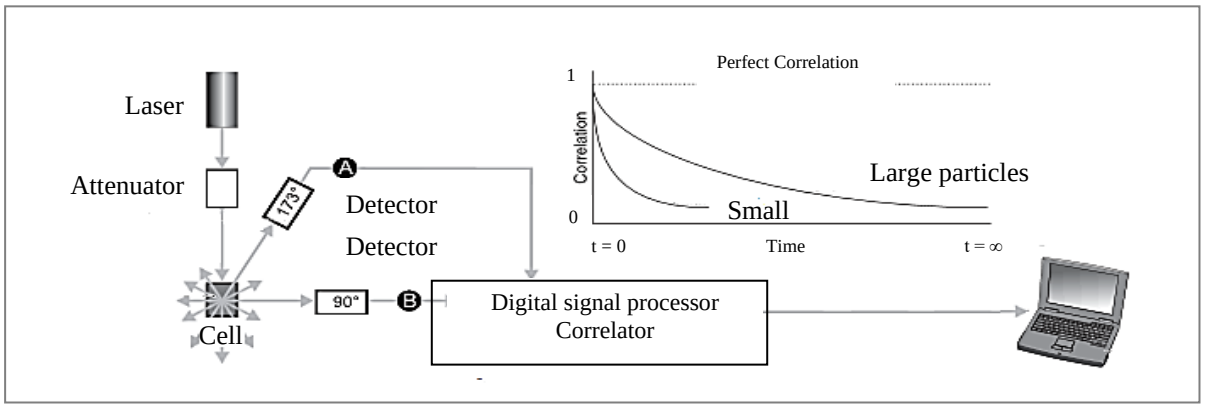

Figure 2. Schematic representation of size measurement system by DLS. Adapted from [6].

APPARATUS

- *ZETASIZER NANO ZS 90 (MALVERN INSTRUMENTS LTD, MALVERN, UK)*

ACCESSORIES AND REAGENTS

AuNPs (diameter: 5-50 nm), β-casein 1 mg/ml in distilled water, 5 M NaCl in distilled water

PREPARATION OF SOLUTIONS AND SAMPLES

AuNPs will be prepared by Turkevich method, treated with NaCl and β-casein solution as described in the Task 4 of the school practice.

EXPERIMENT AND PARAMETERS

1. Turn on PC and Zetasizer Nano, allow the instrument warm up.
2. Double click on DTS Zetasizer software
3. In the File menu, select New, Measurement File, create filename.dts
4. From the Menu Bar select Measure, Manual*. Edit parameters as needed:

Measurement type: **SIZE**

5. Sample: Enter Sample name
6. Material: Select the material you are measuring from the list (Gold nanoparticles), if the material is not listed, you need to enter its refractive index and absorption by yourself (please do not change parameters for the materials that are already in the database)
7. Dispersant: select the solvent from the list / if solvent is not listed you need to enter its viscosity, refractive index and Dielectric constant.
8. Temperature: 25° C
9. Cell: select the proper cell type using the description and Picture.
10. Measurement: Measurement Angle (90°)
    Measurement Duration (Automatic, or Manual: ≈ 12 runs)
    Number of measurements (at least 3)
    Delay (0)
11. Advanced: Accept default values
12. Data processing: General Purpose.
13. Click OK. A measurement window should appear.
14. Click on the Green Start button
15. When measurement is done the instrument will beep once. Saved data will appear on the screen.

When repeating the experiments and using **Manual measurement, be sure that the setting parameters are the same as you have used before. Instead of **Manual** measurement it is also possible to create your **SOP** (standard operation protocol) simplifying routine measurements.*
***Note: Avoid** of **dust** or any **impurities** to be present in your sample. Dispersant/samples should be filtered before measurement (using the appropriately sized filter). Also check the cuvette for possible impurities, when needed flush with deionized water/dispersant (when running the sample of just DI water, the measurement should be aborted).*
For particle sizes smaller than 10 nm, the major factor in determining a minimum concentration is the amount of scattered light that the sample generates. In practice, the concentration should generate a minimum count rate of 10,000 counts per second (10 kcps) in excess of the scattering from the dispersant. As a guide, the scattering from water should give a count rate more than 10 kcps, and toluene more than 100 kcps. Too low concentration will be indicated by the system setting an attenuator index position of 11, and the generated results being variable. In extreme cases, or where there is a bubble in the cell, a 'low sample concentration' error may be displayed. Also check Data quality report/Expert advice.

EVALUATION

Values to be reported will be hydrodynamic diameter expressed as Zeta average size (also known as cumulant mean) together with polydispersity index (PDI). The PDI is dimensionless and scaled such that values smaller than 0.05 are rarely seen other than with highly monodisperse standards. Values greater than 0.7 indicate that the sample has a very broad size distribution and is probably not suitable for the DLS technique.

Size can be analyzed by Intensity distribution (which is fundamental size distribution generated by DLS) as well as by Volume or Number distributions. When transforming an intensity distribution to a volume/number distribution, there are assumptions that must be accepted – sphericity, homogeneity, and the knowledge of the optical properties of the particles. Volume and number distributions derived from intensity distribution are best used for comparative purposes, or for estimating the relative proportions where there are multiple modes, or peaks, and should never be considered absolute. It is therefore good practice to report the size of the peak based on an intensity analysis and report the relative percentages only (not size) from a Volume distribution analysis.

RESULTS

The hydrodynamic sizes (based on Intensity distributions) of AuNPs upon the treatment of NaCl and β-casein will be collected and displayed similarly as illustrated in Figure 3.

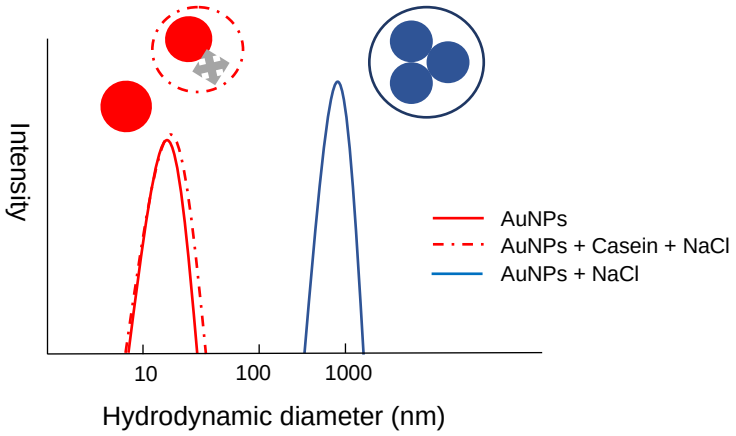

Figure 3. Schematic representation of size measurements by DLS technique. Intensity-weight size distributions of AuNPs – the effect of salt (NaCl) induced formation of larger aggregates and and their prevention by the presence of casein.

REFERENCES

[1] I. Hammami, N.M. Alabdallah, A. Aljomaa, M. Kamoun, Gold nanoparticles: Synthesis properties and applications, J. Of King Saud University - Science 33/7 (2021) 101560.

[2] J. Sun, Y. Lu, L. He, J. Pang, F. Yang, Y. Liu, Colorimetric sensor array based on gold nanoparticles: Design principles and recent advances, TrAC Trends in Analytical Chemistry 122 (2020) 115754.

[3] M. Sun, F. Liu, Y. Zhu, W. Wang, J. Hu, J. Liu, Z. Dai, K. Wang, Y. Wei, J. Bai, W. Gao, Salt-induced aggregation of gold nanoparticles for photoacoustic imaging and photothermal therapy of cancer, Nanoscale 8 (2016) 4452-4457.
[4] Y. Liu, L. Liu, M. Yuan, R. Guo, Preparation, and characterization of casein-stabilized gold nanoparticles for catalytic applications, Colloids and Surfaces A: Physicochemical and Engineering Aspects 417 (2013) 18-25.
[5] T. Zheng, S. Bott, Q. Huo, Techniques for accurate sizing of gold nanoparticles using dynamic light scattering with particular application to chemical and biological sensing based on aggregate formation, ACS Appl. Mater. Interfaces 8/33 (2016) 21585-21594.
[6]http://www.biophysics.bioc.cam.ac.uk/files/Zetasizer_Nano_user_manual_Man0317-1.1.pdf

Edited by

Prof. Tibor Hianik, Faculty of Mathematics, Physics and Informatics, Comenius University in Bratislava, Mlynska dolina F1, 842 48 Bratislava, Slovakia

Reviewers

Prof. Július Cirák, Faculty of Electrical Engineering and Information Technology, Slovak University of Technology in Bratislava, Ilkovičova 3, 81ľ 19 Bratislava, Slovakia

Prof. Martin Weis, Faculty of Electrical Engineering and Information Technology, Slovak University of Technology in Bratislava, Ilkovičova 3, 81ľ 19 Bratislava, Slovakia

Acknowledgments

The publication of this Book of Abstracts was supported by European Union's Horizon 2020 research and innovation programme under the Marie Sklodowska-Curie grant agreement No. 101007299

ISBN 978-80-8147-113-1